Electronic Supplementary Material (ESI) for Catalysis Science & Technology.

Polynuclear Gold (I) Complexes in Photoredox Catalysis: Understanding their Reactivity through Characterization and Kinetic Analysis

C. D. McTiernan, M. Morin, T. McCallum, J. C. Scaiano,* and L. Barriault*

Department of Chemistry and Biomolecular Sciences, Centre for Catalysis Research and Innovation, University of Ottawa, 10 Marie Curie, Ottawa ON K1N 6N5, Canada

*scaiano@photo.chem.uottawa.ca
*lbarriau@uottawa.ca

A. General Information

MeCN, MeOH, *N,N*-diisopropylethylamine (DIPEA), and all other reagents were purchased from commercial suppliers (Sigma Aldrich, Alfa Aesar, and Fisher) and used with no further purification unless otherwise noted.

Light source: Unless otherwise noted, was one UVA (365 nm) LED, which was purchased from LedEngin.

UV-Vis Absorption Spectra: Were recorded on a Cary-100 spectrophotometer, using MeCN as solvent in a 1 cm x 1cm quartz cuvette.

NMR: All ^{1}H and ^{13}C NMR were recorded on a Bruker AVANCE 400 spectrometer. Chemical shifts (δ) are reported in ppm from the solvent.

Optical rotation: Were measured using an Anton Paar MCP 500 Modular Circular Polarimeter at 589 nm with 0.1 dm/2 mL sample cell.

B. General Procedure for the Preparation of Au_x Complexes (GPB)

Phosphine based polynuclear Au(I) complexes were synthesized according to previously described methods [1]. For complexes bearing trifluoromethylsulfonate ($^{-}$OTf) counterions, counterion exchange was performed by addition of AgOTf and filtration to remove AgCl. This was performed to get spectra for complexes 3 and 4. All photocatalysis was performed using the complexes bearing chloride counterions.

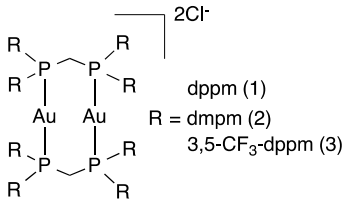

$[Au_2(dppm)_2]Cl_2$ (1)

Synthesized according to GPB and characterized according to previously described methods [1]. ^{31}P NMR were standardized using 85% phosphonic acid as reference.

$[Au_2(dmpm)_2]Cl_2$ (2)

Synthesized according to GPB.

^{1}H NMR: (400 MHz, CD_3OD) δ = 3.05 (quin, *J* = 5.3 Hz, 4 H), 1.83 (td, *J* = 3.8, 1.9 Hz, 24 H) ppm.

^{13}C NMR: (101 MHz, CD_3OD) δ = 31.5 (t, *J* = 15.4 Hz, 2 X CH_2), 14.9 (quin, *J* = 10.3 Hz, 8 X CH_3) ppm.

$[Au_2(3,5\text{-}CF_3\text{-}dppm)_2](OTf)_2$ (3)

Synthesized according to GPB.

^{1}H NMR: (400 MHz, CD_3CN) δ = 8.28 - 8.24 (m, 16 H), 8.23 (br. s, 8 H), 5.04 (quin, *J* = 5.7 Hz, 4 H) ppm.

^{13}C NMR: (101 MHz, CD_3CN) δ = 135.31 (br. s., 16 X CH), 133.58 (quinq, *J* = 34.6, 3.3 Hz, 16 X C), 130.57 (quin, *J* = 16.3 Hz, 8 X C), 128.93 (s, 8 X CH), 123.65 (q, *J* = 274.0 Hz, 16 X C), 121.98 (q, *J* = 320.2 Hz, 2 X C), 26.18 (t, *J* = 15.0 Hz, 2 X CH_2) ppm.

^{31}P NMR: (121MHz, CD_3CN) δ = 40.19 (s, 4 X P) ppm.

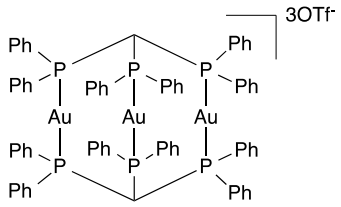

$[Au_3(tppm)_2](OTf)_3$ (4)

Synthesized according to GPB.

^{1}H NMR: (400 MHz, $CDCl_3$) δ = 8.14 (br. s., 24 H), 7.34 (t, *J* = 7.2 Hz, 12 H), 7.26 (t, *J* = 7.2 Hz, 24 H), 2.15 (s, 2 H) ppm.

^{13}C NMR: (101 MHz, $CDCl_3$) δ = 135.5 (24 X CH), 133.9 (12 X CH), 130.0 (24 X CH), 126.6 (12 X C), 30.9 (2 X CH) ppm.

^{31}P NMR: (121MHz, $CDCl_3$) δ = 45.79 (s, 6 X P) ppm.

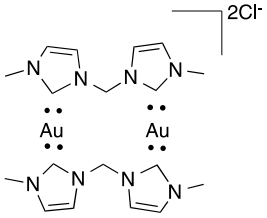

$[Au_2(bmimm)_2]Cl_2$ (5)

$[Au_2(bmimm)_2]Cl_2$ was synthesized using a modified procedure reported by Crabtree[2]. To a high pressure reaction flask (dried, under inert atmosphere, equipped with magnetic stirrer) was added sodium acetate (62 mg, 0.75 mmol, 2.2eq), followed by 1,1'-dimethyl-3,3'-methylene-diimadazolium diiodide (177 mg, 0.41 mmol, 1.2eq) and chloro(dimethylsulfide)gold(I) (100 mg, 0.34 mmol, 1eq). DMF was then added, the reaction vessel capped and heated to 160^{o}C for 1.5 hours. The solution was filtered while still hot (Caution: Let cool to 100^{o}C before opening reaction flask). The filtrate was washed once with DMF, acetone, and diethyl ether. 131mg (94%) of the desired complex was recovered and used as is for photocatalysis without further purification.

^{1}H NMR: (400 MHz, CD_3OD) δ = 7.71 (d, *J* = 1.5 Hz, 4 H), 7.45 (d, *J* = 2.0 Hz, 4 H), 7.20 (d, *J* = 14.0 Hz, 2 H), 6.26 (d, *J* = 14.0 Hz, 2 H), 3.94 (12 H) ppm.

^{13}C NMR: (101MHz, CD_3OD) δ = 185.8 (4 X C), 125.6 (4 X CH), 122.7 (4 X CH), 63.9 (2 X CH_2), 38.9 (4 X CH_3).

C. Procedures for the Preparation of Starting Materials and Products

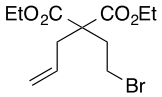

diethyl 2-allyl-2-(2-bromoethyl)malonate (6)
Synthesized according to previously described methods and characterized according to NMR comparison[1].

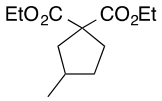

diethyl 3-methylcyclopentane-1,1-dicarboxylate (7a)
Synthesized according to GPD and characterized according to NMR comparison[1].

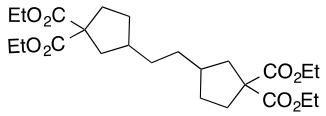

tetraethyl 3,3'-(ethane-1,2-diyl)bis(cyclopentane-1,1-dicarboxylate) (7b)
Synthesized according to GPD.
IR (neat, cm^{-1}): 2981(m), 2938(m), 1730(vs), 1257(s), 1177(m).
^{1}H NMR: (400 MHz, $CDCl_3$) δ = 4.16 (qd, *J* = 7.1, 0.7 Hz, 8 H), 2.42 (dd, *J* = 13.2, 7.1 Hz, 2 H), 2.32 – 2.22 (m, 2 H), 2.16 – 2.06 (m, 2 H), 1.96 – 1.79 (m, 4 H), 1.66 (ddd, *J* = 13.2, 9.9, 1.7 Hz, 2 H), 1.41 – 1.27 (m, 4 H), 1.23 (t, *J* = 7.1 Hz, 14 H, 4 X Ester CH_3's + 2H under t) ppm.
^{13}C NMR: (101 MHz, $CDCl_3$) δ = 172.7 (2 X C), 172.7 (2 X C), 61.2 (4 X CH_2), 59.9 (2 X C), 40.7 (2 X CH_2), 39.9 (2 X CH), 34.1 (2 X CH_2), 33.7 (2 X CH_2), 32.1 (2 X CH_2), 14.0 (4 X CH_3) ppm.
HRMS (EI): *m/z* calc'd for $C_{24}H_{38}O_8$ [M+], 454.2567; found, 454.2560.

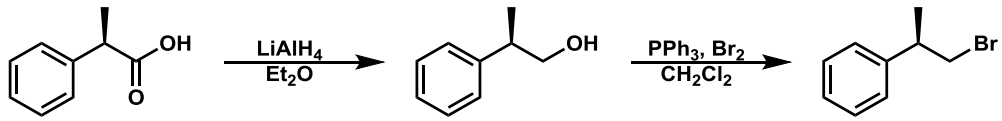

(*R*)-(1-bromopropan-2-yl)benzene (8)
To a flame-dried 100 mL round bottomed flask was added 50 mL of diethyl ether, cooled to 0°C using an ice bath, and added $LiAlH_4$ (15.0 mmol, 3.0 equiv.). (*R*)-(−)-2-phenylpropionic acid (5.0 mmol, 1.0 equiv.) in a minimum of diethyl ether was added dropwise to the solution. The reaction mixture was allowed to warm to room temperature and stirred for 1 hour. Upon completion, the reaction was quenched by slow dropwise addition 0.5 mL of water, then dropwise addition of 0.5 mL of a 15% NaOH aqueous solution, and 1.5 mL of water. This solution was allowed to stir for 30 minutes and was then transferred to a seperatory funnel. The ethereal phase was washed 2 times with a saturated sodium bicarbonate solution, then brine, then dried over sodium sulfate, filtered, concentrated *in vacuo*, and characterized by NMR comparison[3].
To a flame-dried 100 mL round bottomed flask was added PPh_3 (5.5 mmol, 1.1 equiv.) and 50 mL of dichloromethane. The solution was cooled to 0°C using an ice bath and bromine (5.5 mmol, 1.1 equiv.) was added. After stirring for 30 minutes, a white

precipitate formed, indicating the presence of a phosphonium bromide intermediate. (*R*)-2-phenylpropan-1-ol (0.5 mmol, 1.0 equiv.) in a minimum of dichloromethane was added dropwise to this solution, allowed to warm to room temperature, and then refluxed overnight. Upon completion, the solution was added silica, concentrated *in vacuo*, and dry packed upon a flash column. The column was eluted (0%-2% EtOAc:Hexane) where relevant fractions were combined and concentrated *in vacuo*. The product was isolated as an oil (832 mg, 4.2 mmol) with a yield of 84% over both steps and characterized according to NMR comparison [4].
$[\alpha]_D^{23} = +16.6^o$ (c 1.0, $CHCl_3$).

D. General Procedure for the Photocatalyzed Reduction

To an 8 mL pyrex screw-top reaction vessel was added the Au_x complex (0.01 mmol, 0.05 equiv.), bromoalkane (0.20 mmol, 1.00 equiv.), MeCN/MeOH (1:1, 1 mL, 0.2 M), DIPEA (1.00 mmol, 5.00 equiv.) and degassed under argon by sparging. The reaction mixtures were then irradiated with a UVA LED (365 nm) for 0.1-20 hours. The solutions rapidly became dark yellow, red, or brown. Upon reaction completion, the resulting mixtures were concentrated *in vacuo*, and the crude mixtures were placed in a separatory funnel containing EtOAc, washed with 1 M HCl, sat. NaHCO3, and brine, then dried over sodium sulfate, filtered, and concentrated *in vacuo*. The products were analyzed with ^1H and ^{13}C NMR.

E. Absorption Spectra of the Au_x Complexes

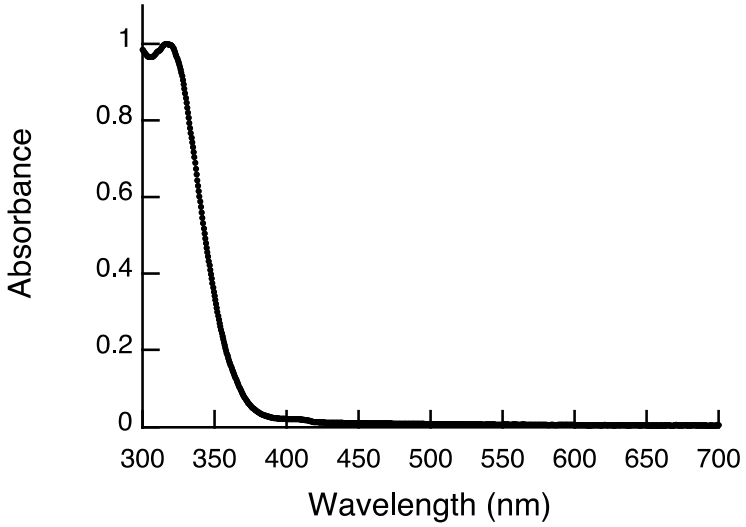

Figure S1. Absorption spectrum of 3.3 $x10^{-3}$ mM $Au_2(dppm)_2Cl_2$ (**1**) in MeCN.

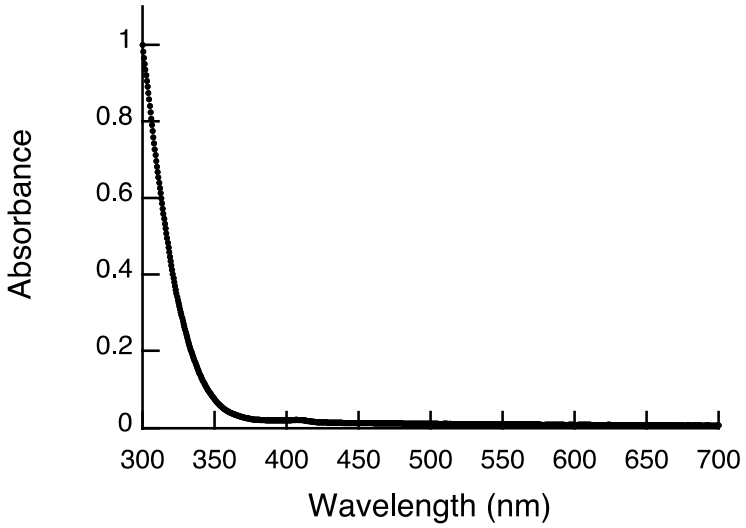

Figure S2. Absorption spectrum of 0.20 mM $Au_2(dmpm)_2Cl_2$ (**2**) in MeCN.

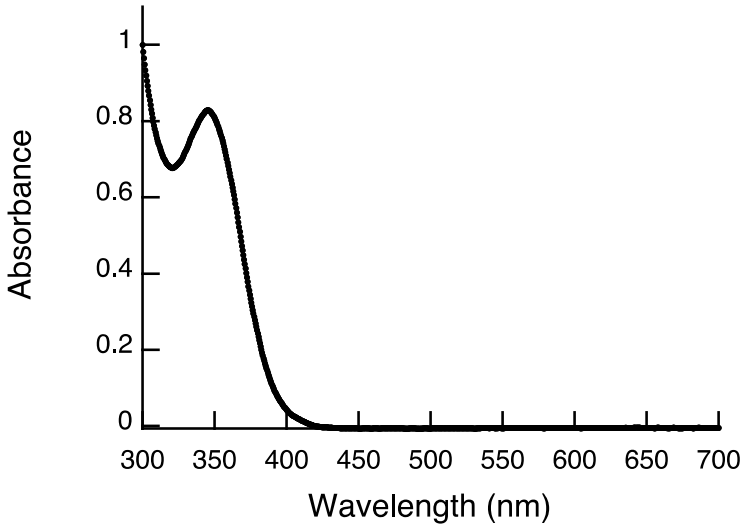

Figure S3. Absorption spectrum of 0.12 mM $Au_2(3,5\text{-}CF_3\text{-}dppm)_2Cl_2$ (**3**) in MeCN.

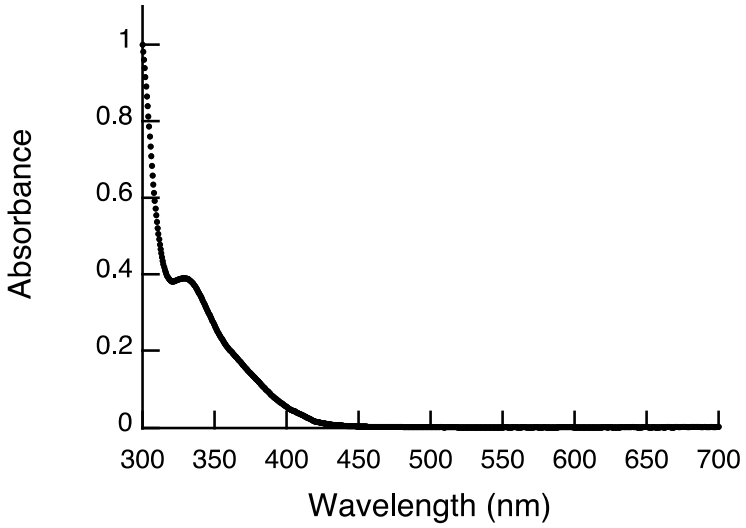

Figure S4. Absorption spectrum of 6.1 x 10^{-2} mM $Au_2(tppm)_2Cl_2$ (**4**) in MeCN.

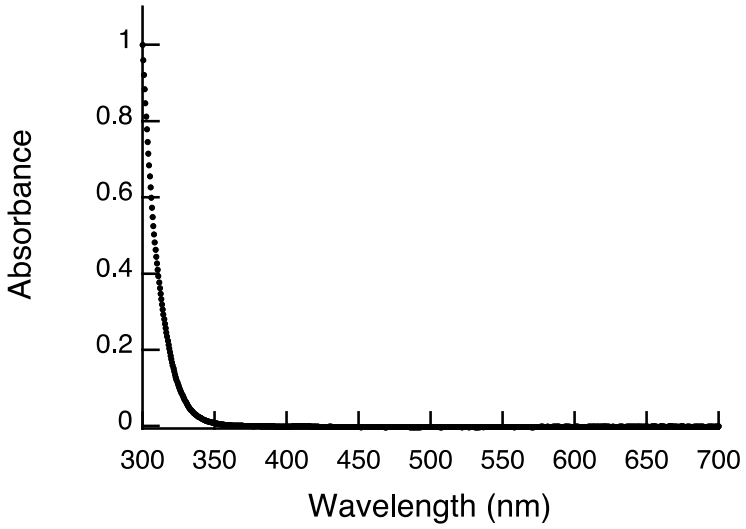

Figure S5. Absorption spectrum of 1.02 mM $Au_2(bmimm)_2Cl_2$ (**5**) in MeCN.

F. 77 K Phosphorescence Spectra of the Au_x Complexes
Determination of Triplet Energies (E^*_T)

The low temperature phosphorescence measurements, from which the triplet energy of the Au_x complexes was determined, were carried out in a Photon Technology International (PTI) spectrofluorimeter. Cooling to 77K was accomplished using a quartz cold finger and liquid N_2. Spectra of the Au_x complexes were recorded from ethanol:methanol (1:1) glass in a quartz EPR tube. None of the emission spectra of the Au_x complexes exhibited fine structure. Therefore we have estimated the energy of the $(0\text{-}0)_{T\text{-}S}$ transition from the emission maxima. This most likely results in the triplet energy value being underestimated.

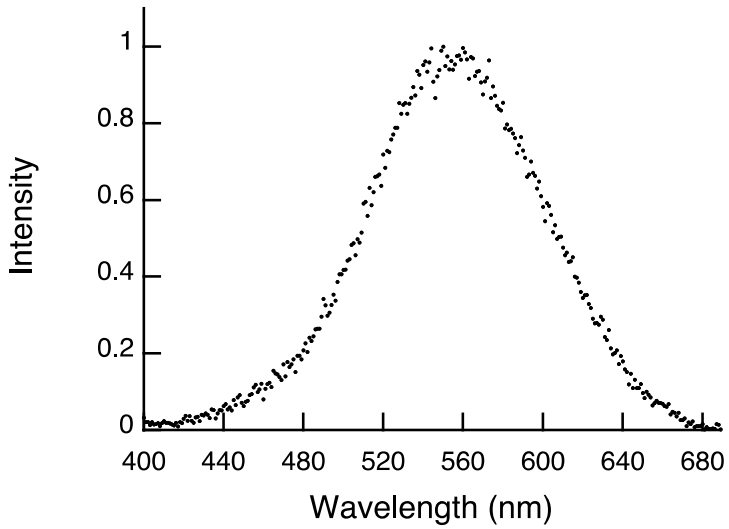

Figure S6. 77 K phosphorescence spectrum of $Au_2(dppm)_2Cl_2$ (**1**) in EtOH:MeOH glass.

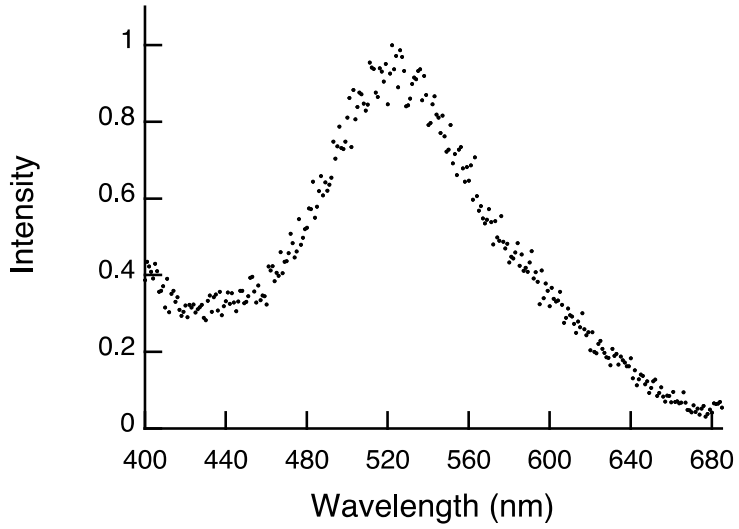

Figure S7. 77 K phosphorescence spectrum of $Au_2(dmpm)_2Cl_2$ (**2**) in EtOH:MeOH glass.

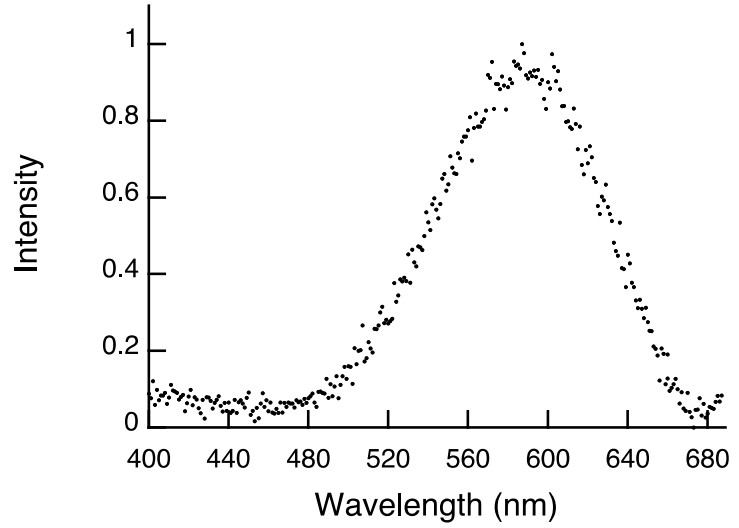

Figure S8. 77 K phosphorescence spectrum of $Au_2(3,5\text{-}CF_3\text{-}dppm)_2Cl_2$ (**3**) in EtOH:MeOH glass.

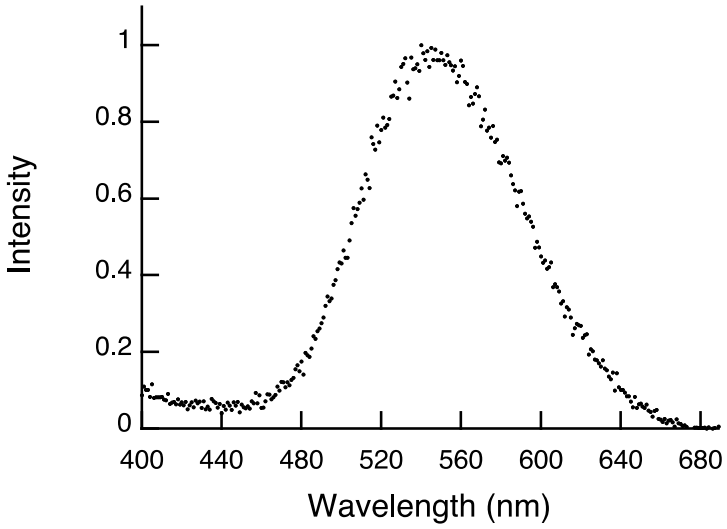

Figure S9. 77 K phosphorescence spectrum of $Au_2(tppm)_2Cl_2$ (**4**) in EtOH:MeOH glass.

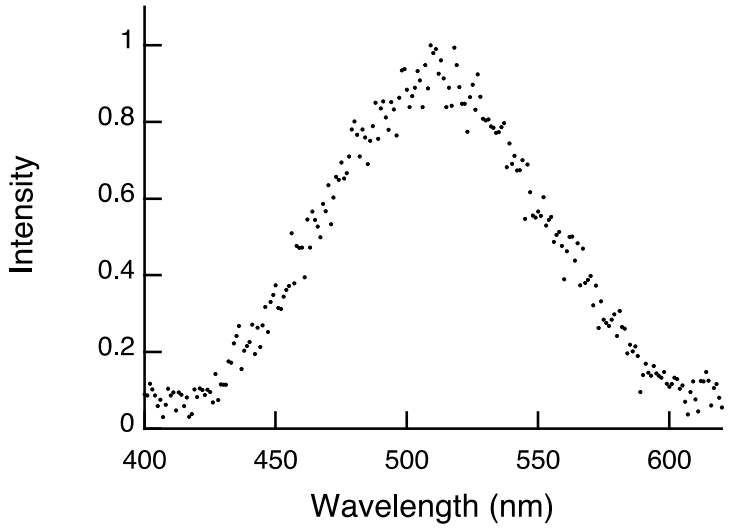

Figure S10. 77 K phosphorescence spectrum of $Au_2(bmimm)_2Cl_2$ (**5**) in EtOH:MeOH glass.

G. Laser Flash Photolysis Data of the Au_x Complexes

Experiments were performed using either a Q-switched Nd:YAG-laser (355 nm, 10 mJ/pulse) or an excimer laser (308 nm, 10 mJ/pulse) in a LFP-111 laser-flash photolysis (LFP) system (Luzchem Research Inc., Ottawa, Canada) and 1 cm x 1 cm quartz cuvette (Luzchem). Samples of the Au_x complexes were prepared in MeCN with a total volume of 3 mL and an absorbance of ~0.1 at 308 or 355 nm. The samples were degasses with N_2 for 30 minutes prior to use. The substrates used in the quenching studies were also prepared in MeCN and were degassed for the duration of the experiment.

$Au_2(dppm)_2Cl_2$ (1)

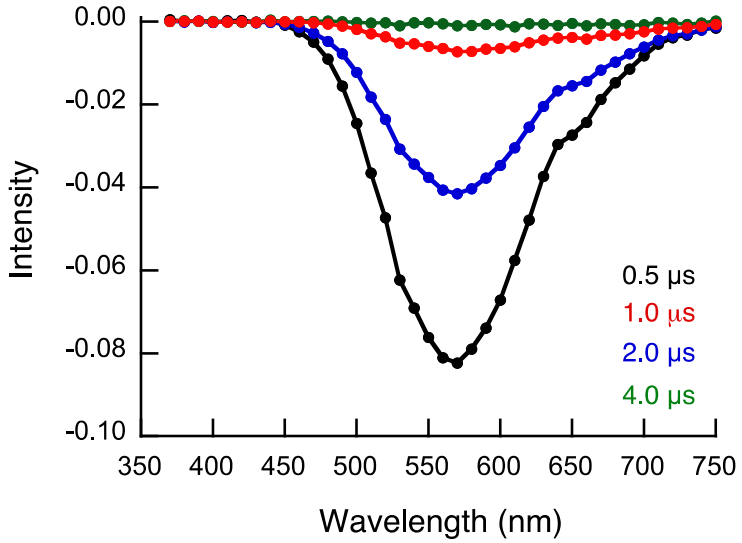

Figure S11. Transient emission spectrum showing the $^3Au_2(dppm)_2Cl_2$ signal obtained upon laser pulse excitation (355 nm, 10 mJ) of a $Au_2(dppm)_2Cl_2$ sample which had been purged of oxygen.

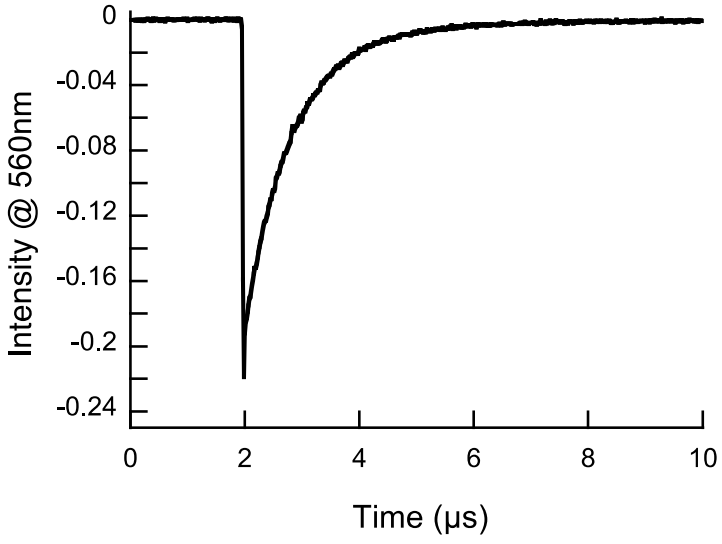

Figure S12. Decay trace of $^3Au_2(dppm)_2Cl_2$ at 560 nm obtained upon laser pulse excitation (355 nm, 10 mJ) of a $Au_2(dppm)_2Cl_2$ sample which had been purged of oxygen.

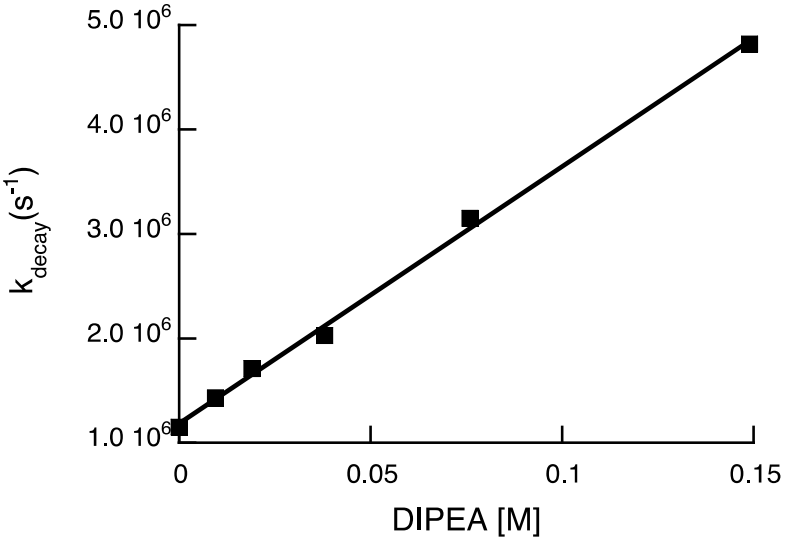

Figure S13. Kinetic quenching plot showing the quenching of $^3Au_2(dppm)_2Cl_2$ by DIPEA. The slope of this plot corresponds to bimolecular rate constant.

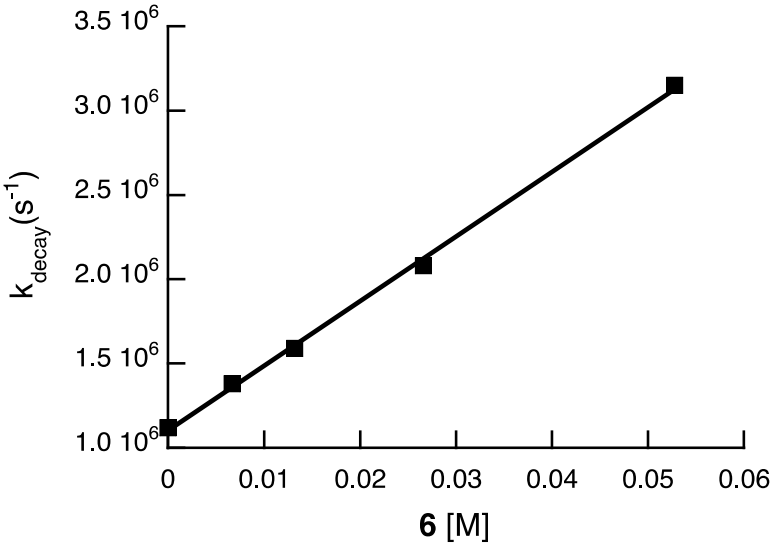

Figure S14. Kinetic quenching plot showing the quenching of $^3Au_2(dppm)_2Cl_2$ by substrate **6**. The slope of this plot corresponds to bimolecular rate constant.

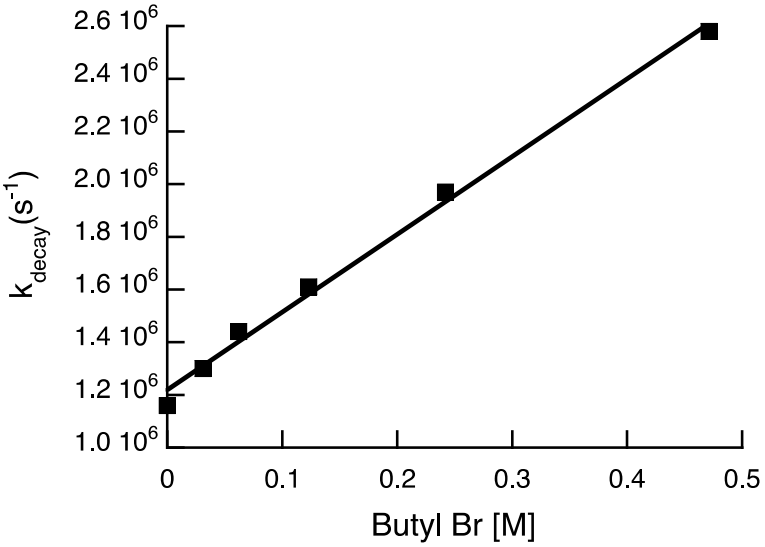

Figure S15. Kinetic quenching plot showing the quenching of $^{3}Au_2(dppm)_2Cl_2$ by butyl bromide. The slope of this plot corresponds to bimolecular rate constant.

$Au_2(dmpm)_2Cl_2$ (2)

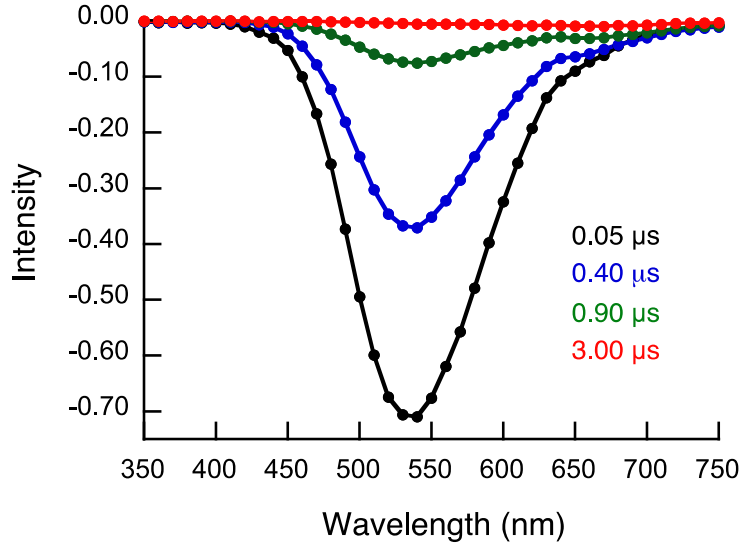

Figure S16. Transient emission spectrum showing the $^{3}Au_2(dmpm)_2Cl_2$ signal obtained upon laser pulse excitation (308 nm, 10 mJ) of a $Au_2(dmpm)_2Cl_2$ sample which had been purged of oxygen.

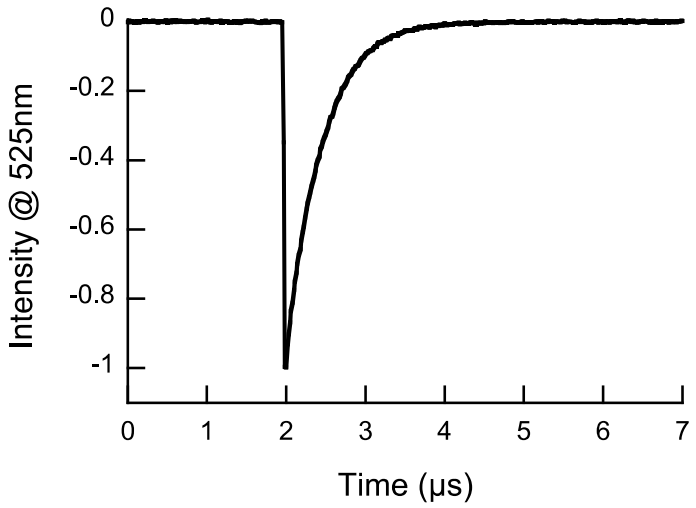

Figure S17. Decay trace of $^3Au_2(dmpm)_2Cl_2$ at 525 nm obtained upon laser pulse excitation (308 nm, 10 mJ) of a $Au_2(dmpm)_2Cl_2$ sample which had been purged of oxygen.

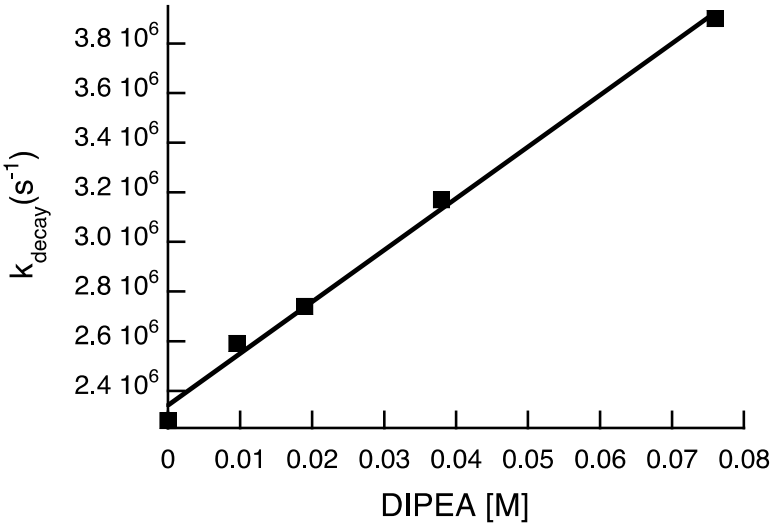

Figure S18. Kinetic quenching plot showing the quenching of $^3Au_2(dmpm)_2Cl_2$ by DIPEA. The slope of this plot corresponds to bimolecular rate constant

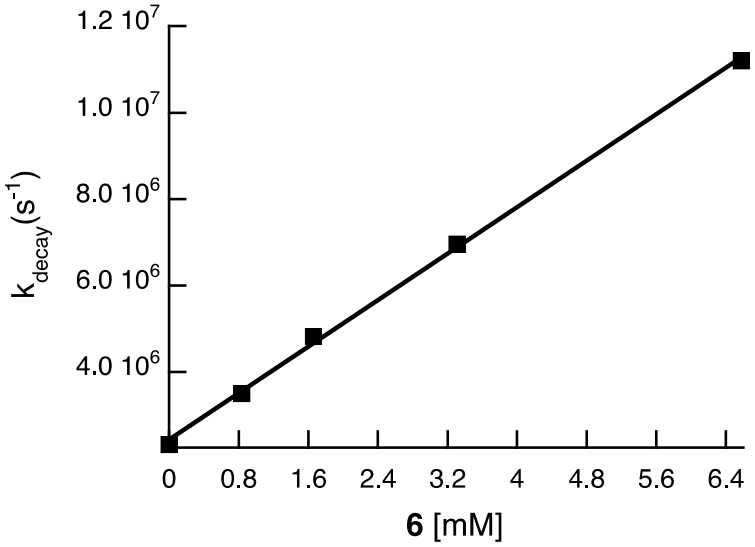

Figure S19. Kinetic quenching plot showing the quenching of $^3Au_2(dmpm)_2Cl_2$ by substrate **6**. The slope of this plot corresponds to bimolecular rate constant.

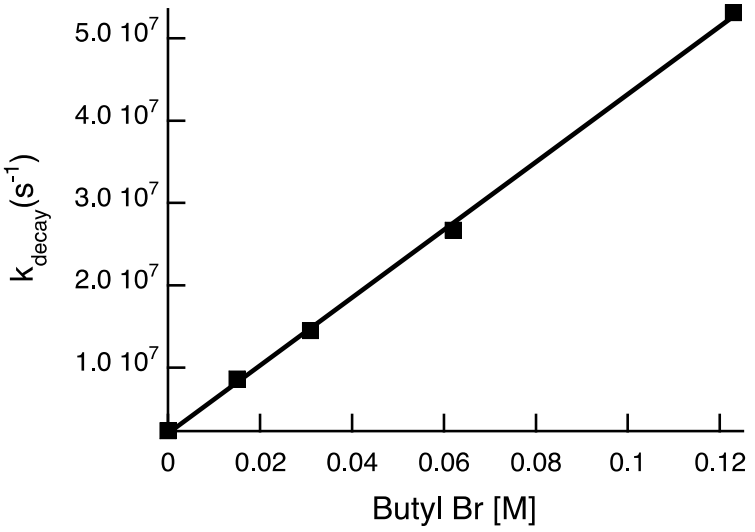

Figure S20. Kinetic quenching plot showing the quenching of $^3Au_2(dmpm)_2Cl_2$ by butyl bromide. The slope of this plot corresponds to bimolecular rate constant.

$Au_2(3,5\text{-}CF_3\text{-}dppm)_2Cl_2$ (3)

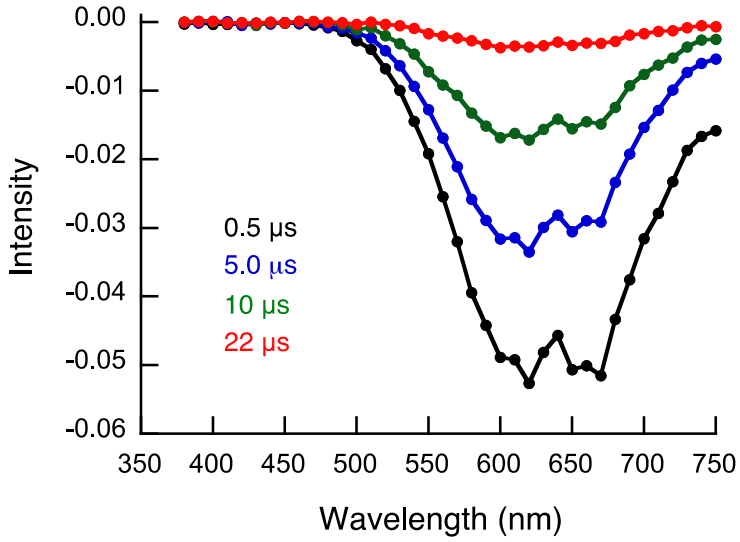

Figure S21. Transient emission spectrum showing the $^3Au_2(3,5\text{-}CF_3\text{-}dppm)_2Cl_2$ signal obtained upon laser pulse excitation (355 nm, 10 mJ) of a $Au_2(3,5\text{-}CF_3\text{-}dppm)_2Cl_2$ sample which had been purged of oxygen.

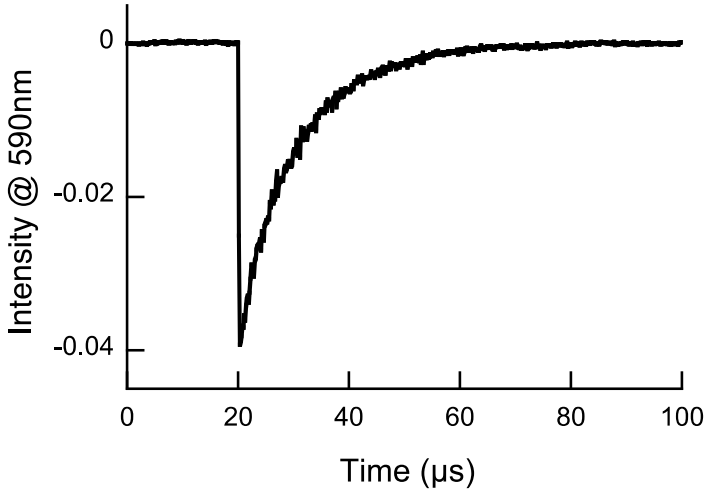

Figure S22. Decay trace of $^3Au_2(3,5\text{-}CF_3\text{-}dppm)_2Cl_2$ at 590 nm obtained upon laser pulse excitation (355 nm, 10 mJ) of a $Au_2(3,5\text{-}CF_3\text{-}dppm)_2Cl_2$ sample which had been purged of oxygen.

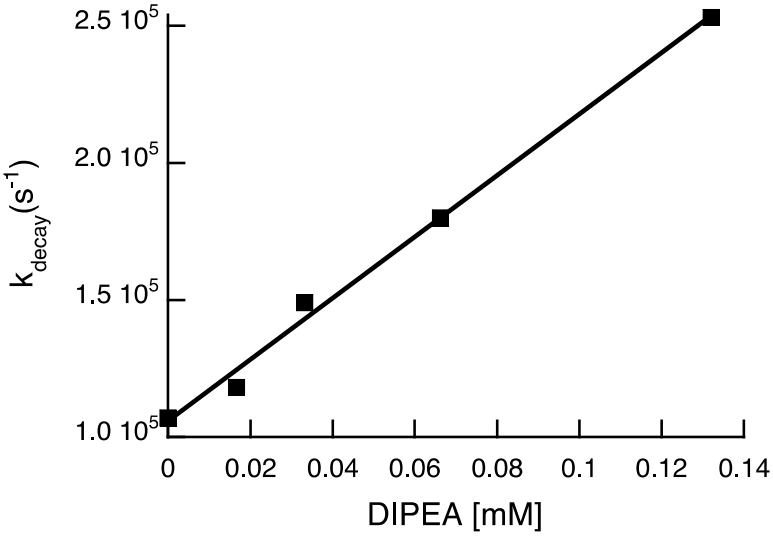

Figure S23. Kinetic quenching plot showing the quenching of $^{3}Au_2(3,5\text{-}CF_3\text{-}dppm)_2Cl_2$ by DIPEA. The slope of this plot corresponds to bimolecular rate constant.

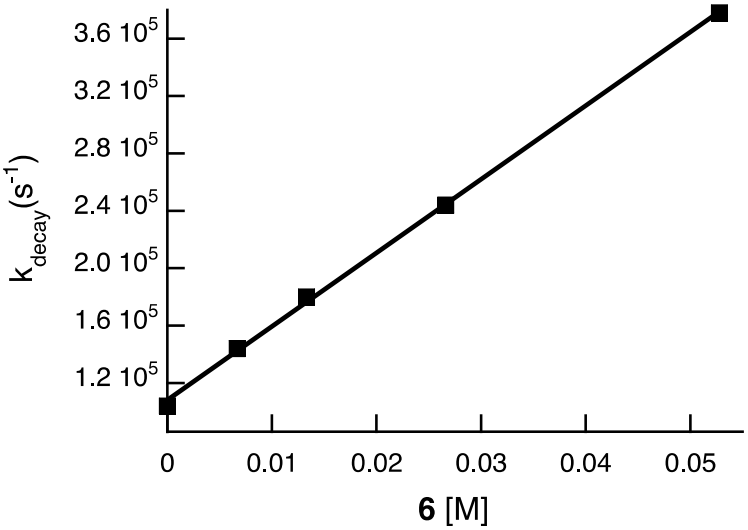

Figure S24. Kinetic quenching plot showing the quenching of $^{3}Au_2(3,5\text{-}CF_3\text{-}dppm)_2Cl_2$ by substrate **6**. The slope of this plot corresponds to bimolecular rate constant.

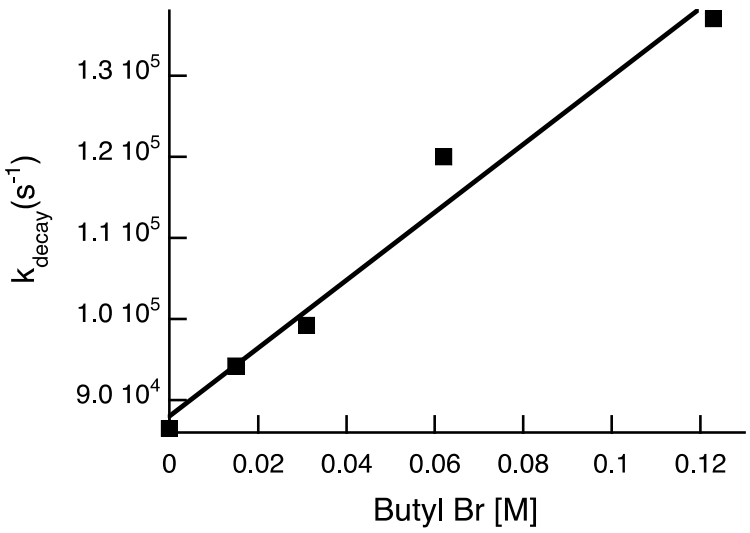

Figure S25. Kinetic quenching plot showing the quenching of $^{3}Au_2(3,5\text{-}CF_3\text{-}dppm)_2Cl_2$ by butyl bromide. The slope of this plot corresponds to bimolecular rate constant.

$Au_2(tppm)_2Cl_2$ (4)

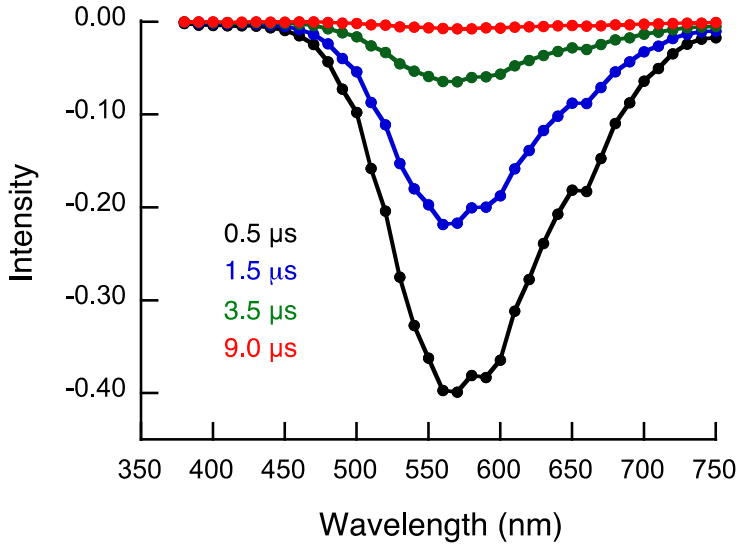

Figure S26. Transient emission spectrum showing the $^{3}Au_2(tppm)_2Cl_2$ signal obtained upon laser pulse excitation (355 nm, 10 mJ) of a $Au_2(tppm)_2Cl_2$ sample which had been purged of oxygen.

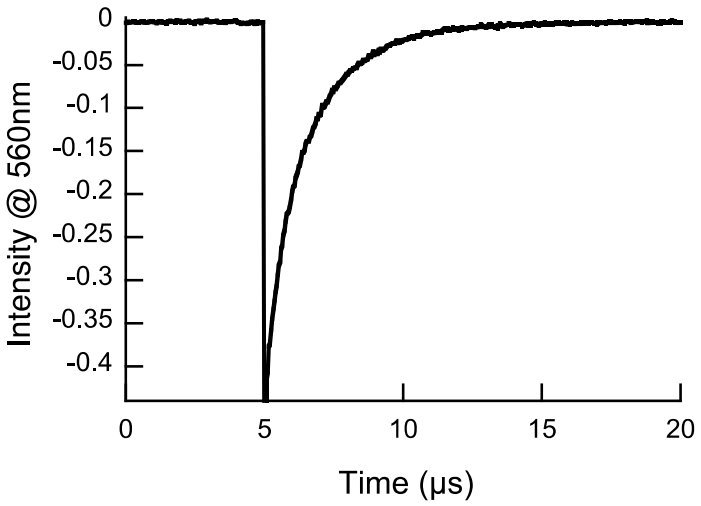

Figure S27. Decay trace of $^3Au_2(tppm)_2Cl_2$ at 560 nm obtained upon laser pulse excitation (355 nm, 10 mJ) of a $Au_2(tppm)_2Cl_2$ sample which had been purged of oxygen.

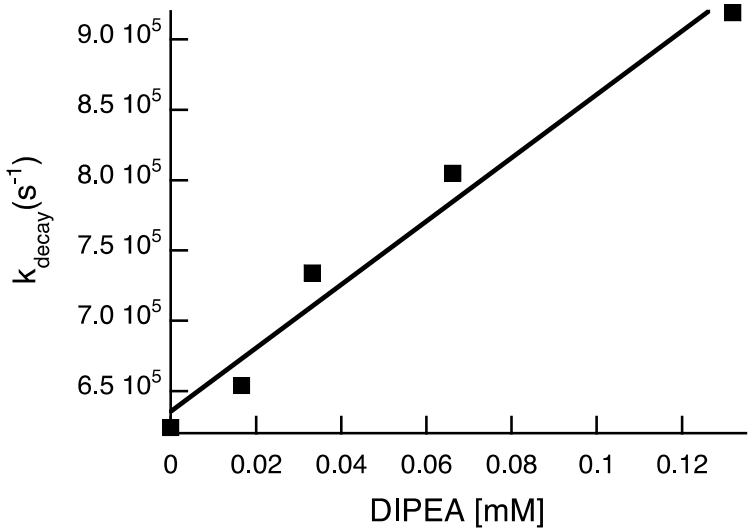

Figure S28. Kinetic quenching plot showing the quenching of $^3Au_2(tppm)_2Cl_2$ by DIPEA. The slope of this plot corresponds to bimolecular rate constant.

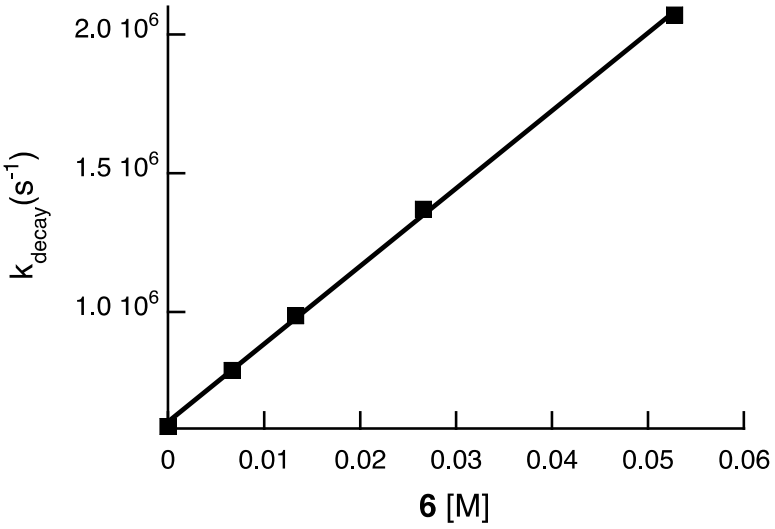

Figure S29. Kinetic quenching plot showing the quenching of $^3Au_2(tppm)_2Cl_2$ by substrate **6**. The slope of this plot corresponds to bimolecular rate constant.

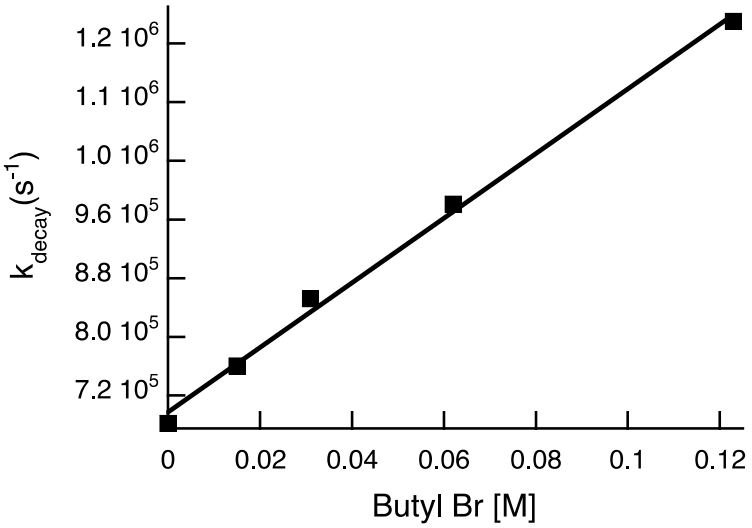

Figure S30. Kinetic quenching plot showing the quenching of $^3Au_2(tppm)_2Cl_2$ by butyl bromide. The slope of this plot corresponds to bimolecular rate constant.

$Au_2(bmimm)_2Cl_2$ (5)

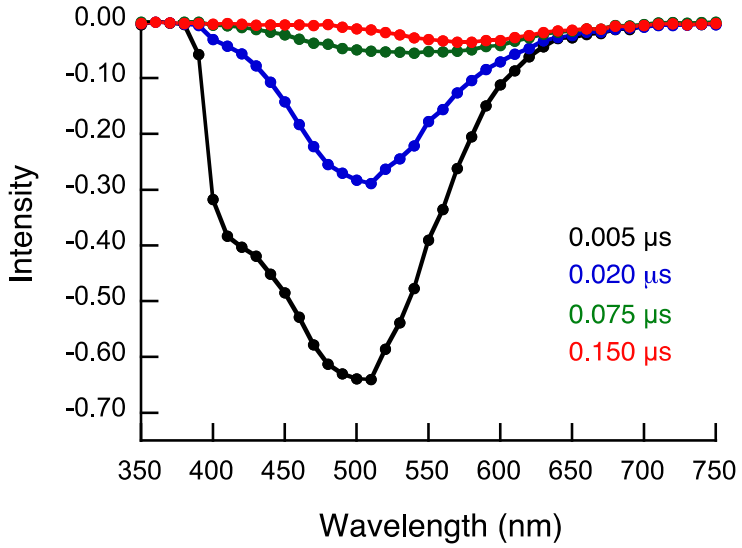

Figure S31. Transient emission spectrum showing the $^3Au_2(bmimm)_2Cl_2$ signal obtained upon laser pulse excitation (308 nm, 10 mJ) of a $Au_2(bmimm)_2Cl_2$ sample which had been purged of oxygen.

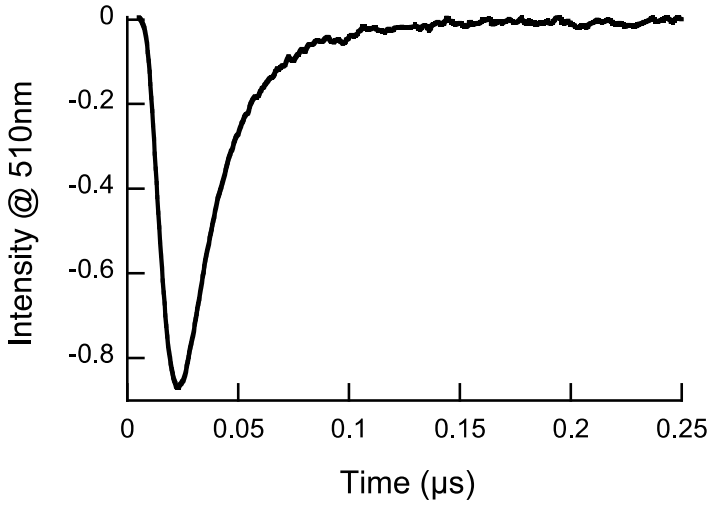

Figure S32. Decay trace of $^3Au_2(bmimm)_2Cl_2$ at 510 nm obtained upon laser pulse excitation (308 nm, 10 mJ) of a $Au_2(bmimm)_2Cl_2$ sample which had been purged of oxygen.

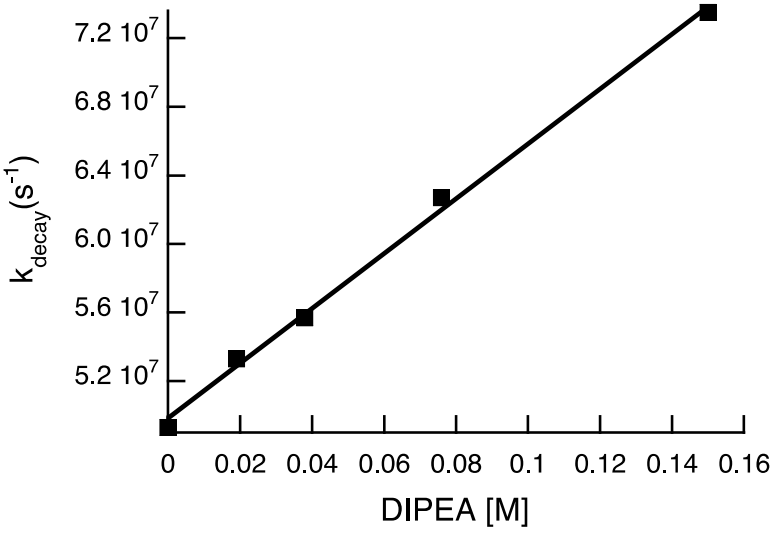

Figure S33. Kinetic quenching plot showing the quenching of $^3Au_2(bmimm)_2Cl_2$ by DIPEA. The slope of this plot corresponds to bimolecular rate constant.

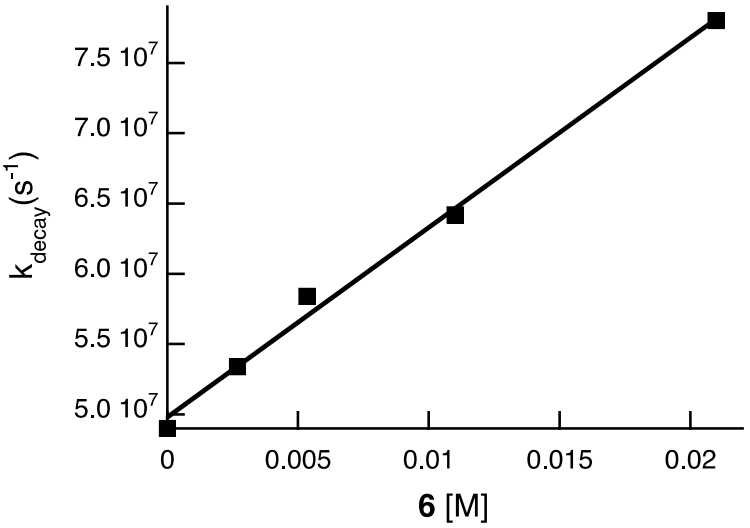

Figure S34. Kinetic quenching plot showing the quenching of $^3Au_2(bmimm)_2Cl_2$ by substrate **6**. The slope of this plot corresponds to bimolecular rate constant.

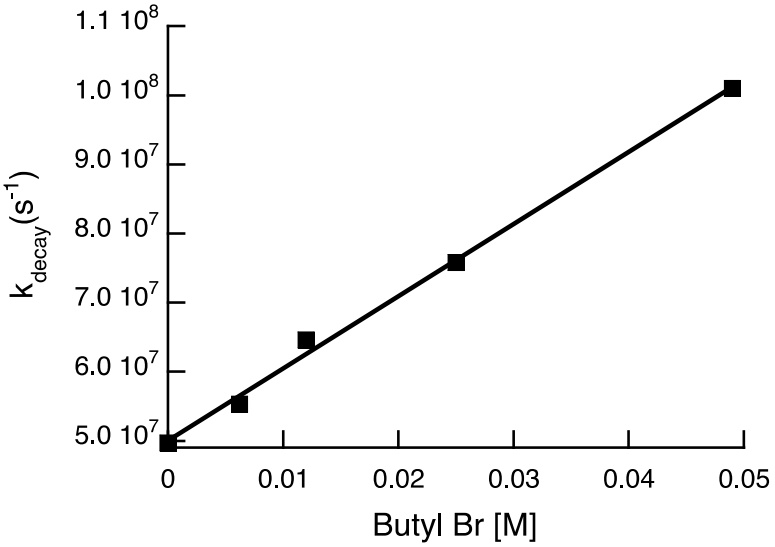

Figure S35. Kinetic quenching plot showing the quenching of $^3Au_2(bmimm)_2Cl_2$ by butyl bromide. The slope of this plot corresponds to bimolecular rate constant.

H. Cyclic Voltammetry Measurements of the Au_x Complexes

Conditions for cyclic voltammetry measurements: scan rate = 100 mV s^{-1}; 0.5-2.0 mM Au (I) complex in Ar degassed MeCN containing 100 mM Bu_4NclO_4 supporting electrolyte; Pt wire working electrode; Pt wire counter electrode; Ag wire pseudo-reference electrode; Fc/Fc^+ redox couple as internal reference (0.41 V vs. SCE); oxidation and reduction potential reported as peak anodic (E_{pa}) and peak cathodic (E_{pc}) potentials due to their irreversible nature.

$Au_2(dppm)_2Cl_2$ (1)

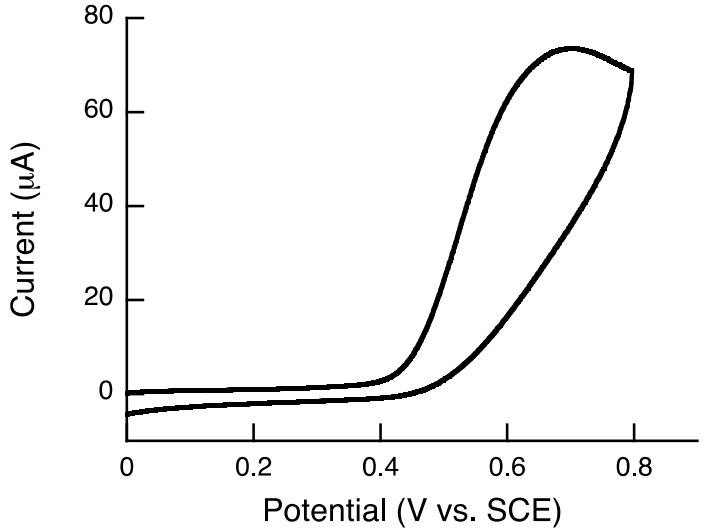

Figure S36. Cyclic voltammogram of $Au_2(dppm)_2Cl_2$ [Anodic Scan].

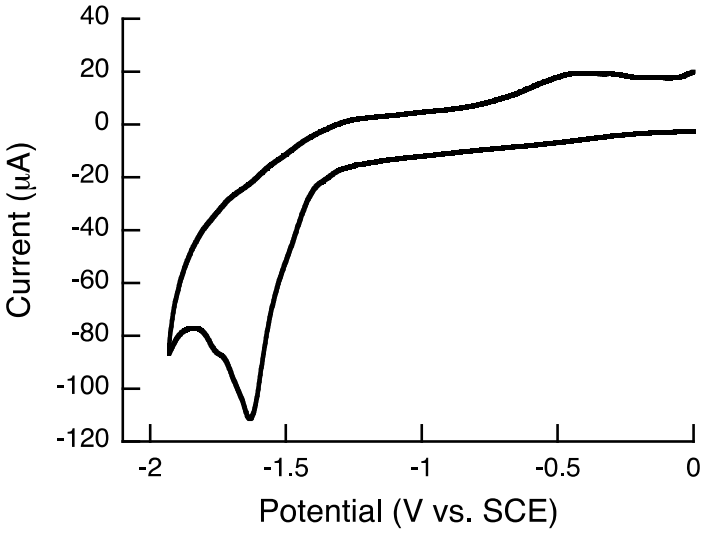

Figure S37. Cyclic voltammogram of $Au_2(dppm)_2Cl_2$ [Cathodic Scan].

$Au_2(dmpm)_2Cl_2$ (2)

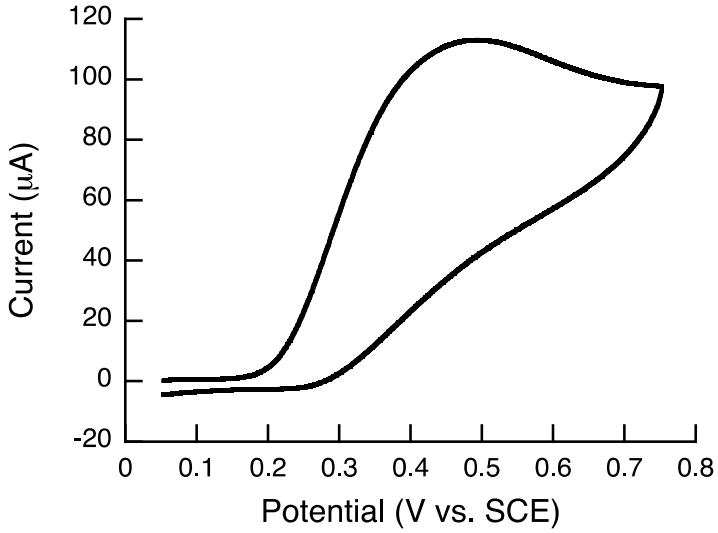

Figure S38. Cyclic voltammogram of $Au_2(dmpm)_2Cl_2$ [Anodic Scan].

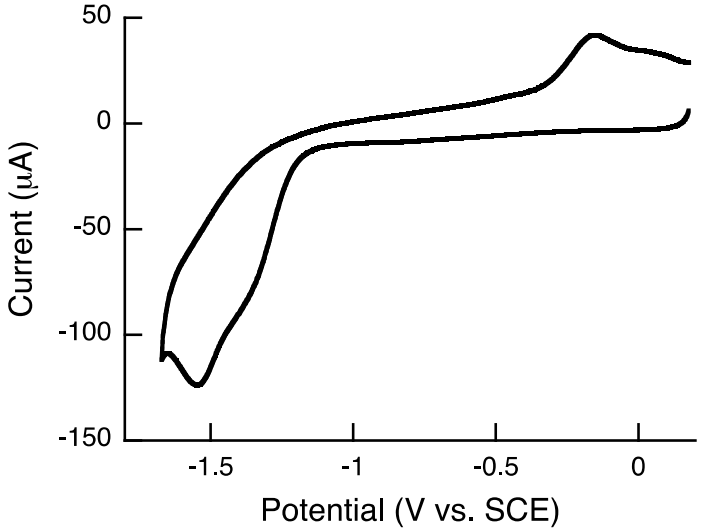

Figure S39. Cyclic voltammogram of $Au_2(dmpm)_2Cl_2$ [Cathodic Scan].

Au_2(3,5-CF_3-dppm)$_2Cl_2$ (3)

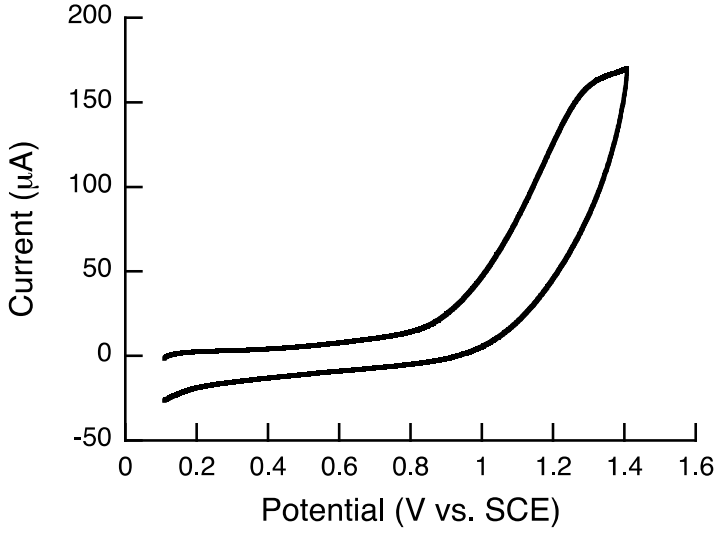

Figure S40. Cyclic voltammogram of Au_2(3,5-CF_3-dppm)$_2Cl_2$ [Anodic Scan].

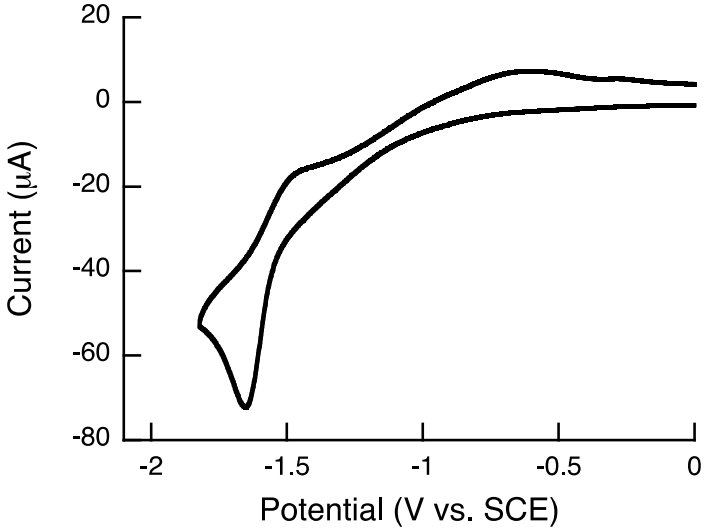

Figure S41. Cyclic voltammogram of Au_2(3,5-CF_3-dppm)$_2Cl_2$ [Cathodic Scan].

$Au_2(tppm)_2Cl_2$ (4)

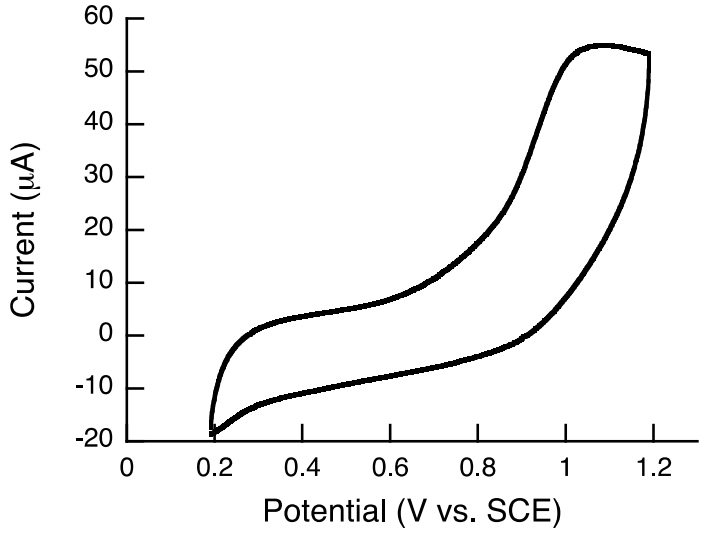

Figure S42. Cyclic voltammogram of $Au_2(tppm)_2Cl_2$ [Anodic Scan].

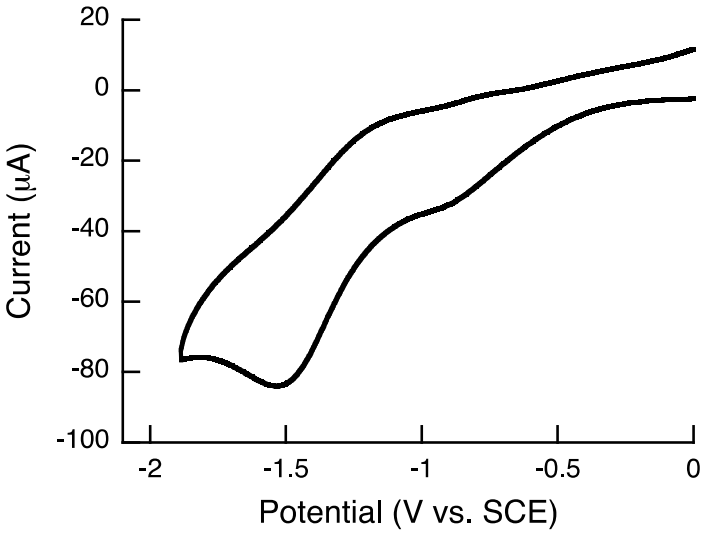

Figure S43. Cyclic voltammogram of $Au_2(tppm)_2Cl_2$ [Cathodic Scan].

$Au_2(bmimm)_2Cl_2$ (5)

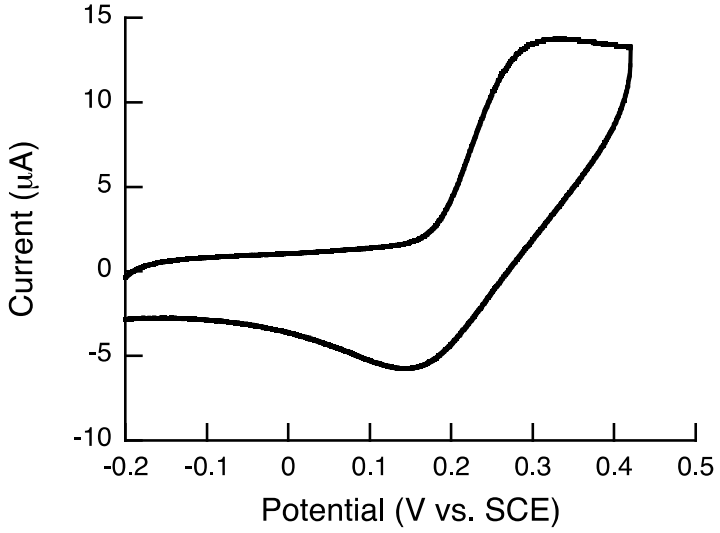

Figure S44. Cyclic voltammogram of $Au_2(bmimm)_2Cl_2$ [Anodic Scan].

Calculating the excited state redox potentials of the Au_x complexes: Using the triplet energy (E^*_T) and ground state oxidation (E_{pa}) and reduction (E_{pc}) potentials of the Au_x complexes we can determine their corresponding excited state oxidation (E^*_{ox}) and reduction (E^*_{red}) potentials using the following equations:

$$E^*_{ox} = E_{pa} - E^*_T$$

$$E^*_{red} = E_{pc} + E^*_T$$

Table S1. Excited State Redox Potentials of the Polynuclear Gold (I) Complexes.

Catalyst	E^*_T (V)	E_{pa} (V vs SCE)	E_{pc} (V vs SCE)	E^*_{ox} (V vs SCE)	E^*_{red} (V vs SCE)
(**1**) $Au_2(dppm)_2Cl_2$	2.23	0.70	-1.63	-1.53	0.60
(**2**) $Au_2(dmpm)_2Cl_2$	2.36	0.49	-1.77	-1.87	0.59
(**3**) $Au_2(3,5\text{-}CF_3\text{-}dppm)_2Cl_2$	2.10	1.41	-1.65	-0.69	0.45
(**4**) $Au_3(tppm)_3Cl_3$	2.28	1.09	-1.54	-1.19	0.74
(**5**) $Au_2(bmimm)_2Cl_2$	2.44	0.34	-	-2.10	-

I. Power Spectrum of 365 nm LED

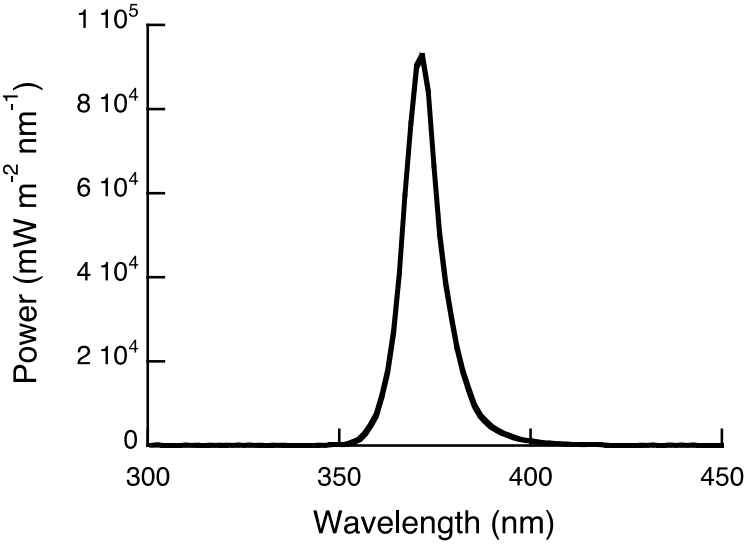

Figure S45. Spectral power of the 365 nm LED (LZ4-40U600)

J. References

[1] Revol, G.; McCallum, T.; Morin, M.; Gagosz, F.; Barriault, L. *Angew. Chem., Int. Ed.* **2013**, *52*, 13342.

[2] Poyatos, M.; McNamara, W.; Incarvito, C.; Peris, E.; Crabtree, R. H. *Chem. Commun*., **2007**, 2267.

[3] Szostak, M.; Spain, M.; Eberhart, A. J.; Procter, D. J. *J. Org. Chem*. **2014**, *79*, 11988.

[4] Prins, L. J.; Hulst, R.; Timmerman, P.; Reinhoudt, D. N. *Chem. Eur. J*. **2002**, *8*, 2288.

K. NMR Spectra

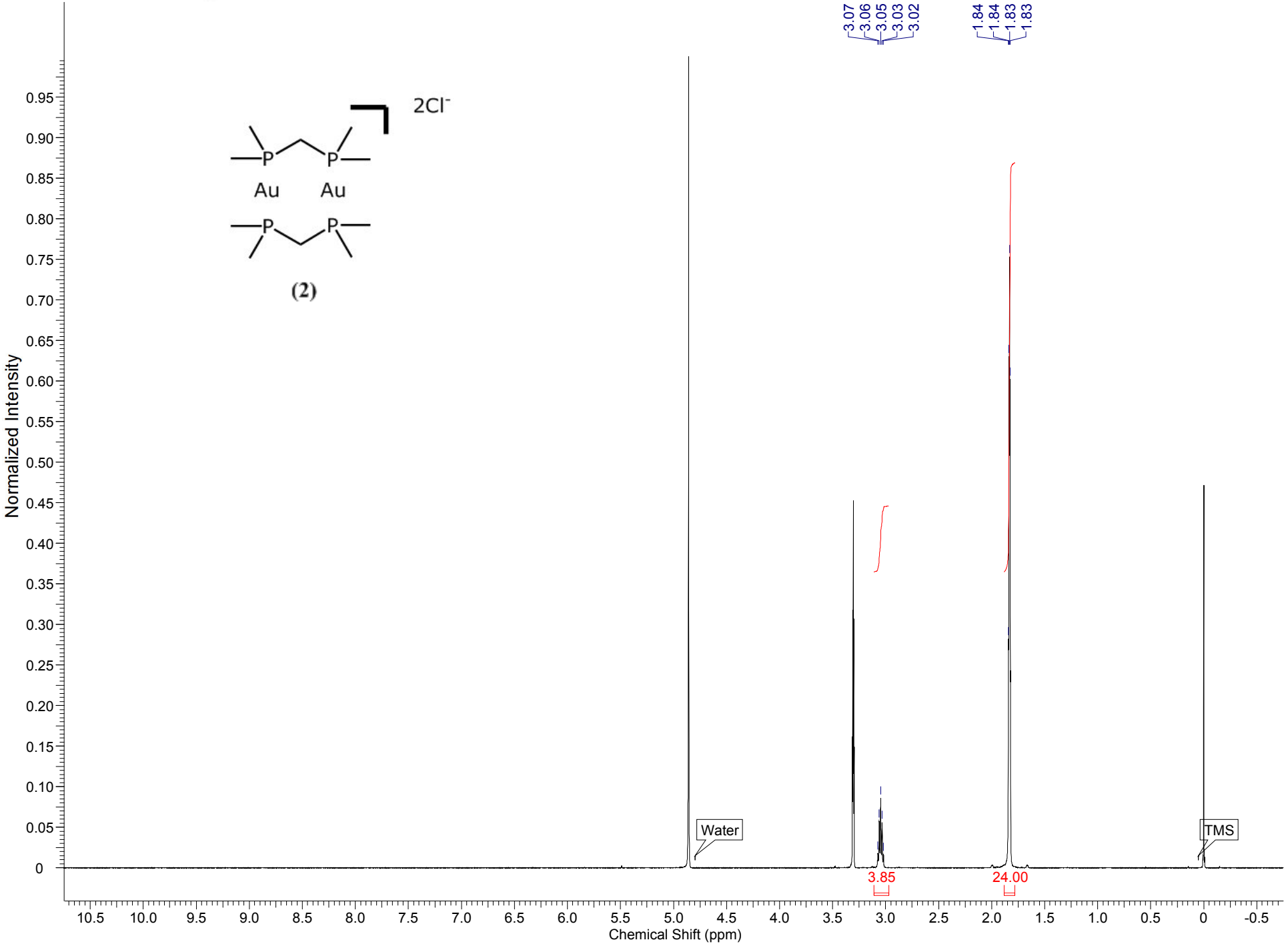

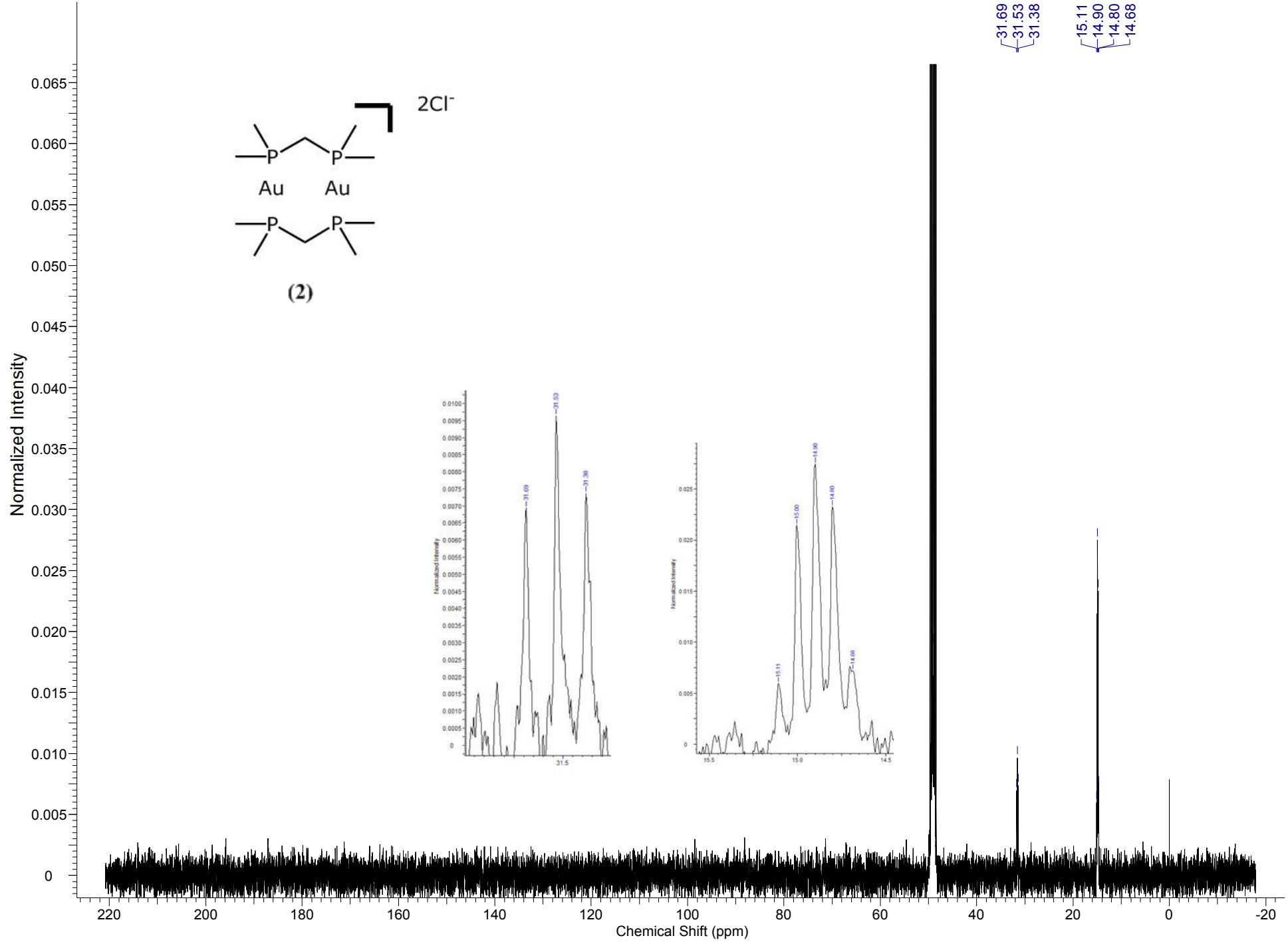
31.69
31.53
31.38
15.11
14.90
14.80
14.68
2Cl⁻
P
P
Au
Au
P
P
(2)
Normalized Intensity
Chemical Shift (ppm)
0.065
0.060
0.055
0.050
0.045
0.040
0.035
0.030
0.025
0.020
0.015
0.010
0.005
0
220
200
180
160
140
120
100
80
60
40
20
0
-20

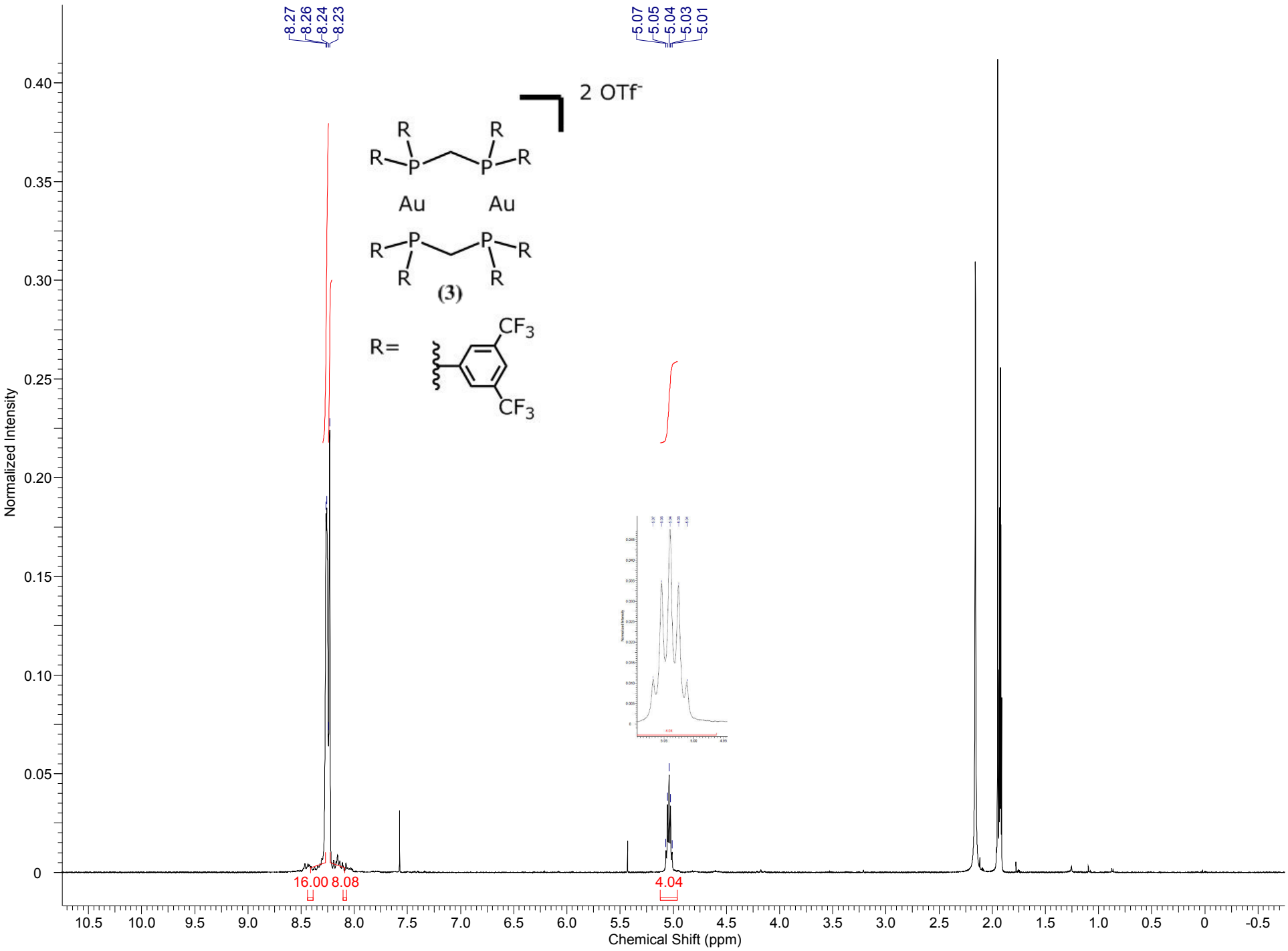
8.27
8.26
8.24
8.23
5.07
5.05
5.04
5.03
5.01
2 OTf-
R
P
Au
(3)
R=
CF3
Normalized Intensity
0.40
0.35
0.30
0.25
0.20
0.15
0.10
0.05
0
16.00
8.08
4.04
10.5
10.0
9.5
9.0
8.5
8.0
7.5
7.0
6.5
6.0
5.5
5.0
4.5
4.0
3.5
3.0
2.5
2.0
1.5
1.0
0.5
0
-0.5
Chemical Shift (ppm)

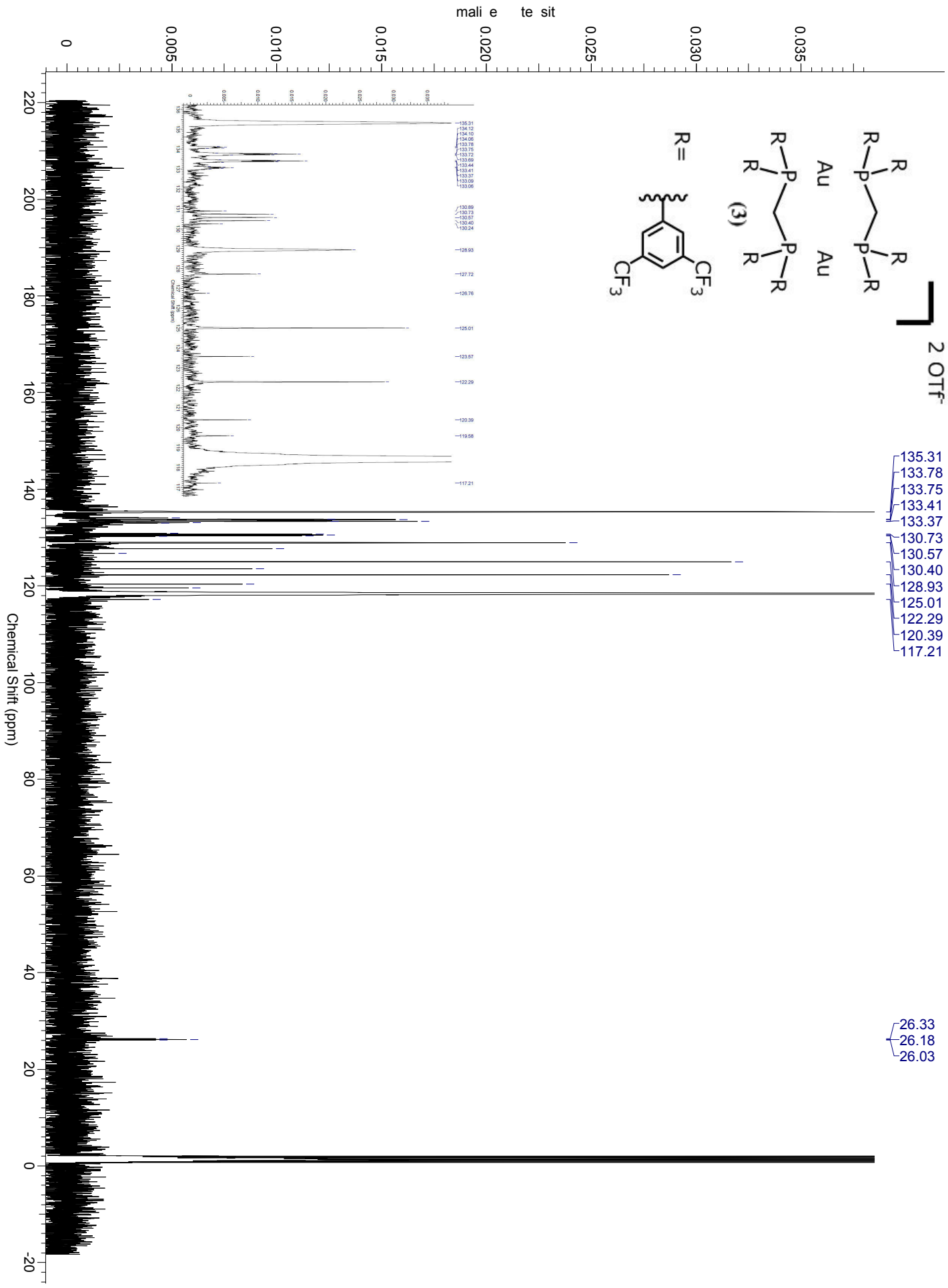
mali e te sit
0
0.005
0.010
0.015
0.020
0.025
0.030
0.035
Chemical Shift (ppm)
220
200
180
160
140
120
100
80
60
40
20
0
-20
135.31
133.78
133.75
133.41
133.37
130.73
130.57
130.40
128.93
125.01
122.29
120.39
117.21
26.33
26.18
26.03
R=
CF3
CF3
(3)
Au
Au
2 OTf-

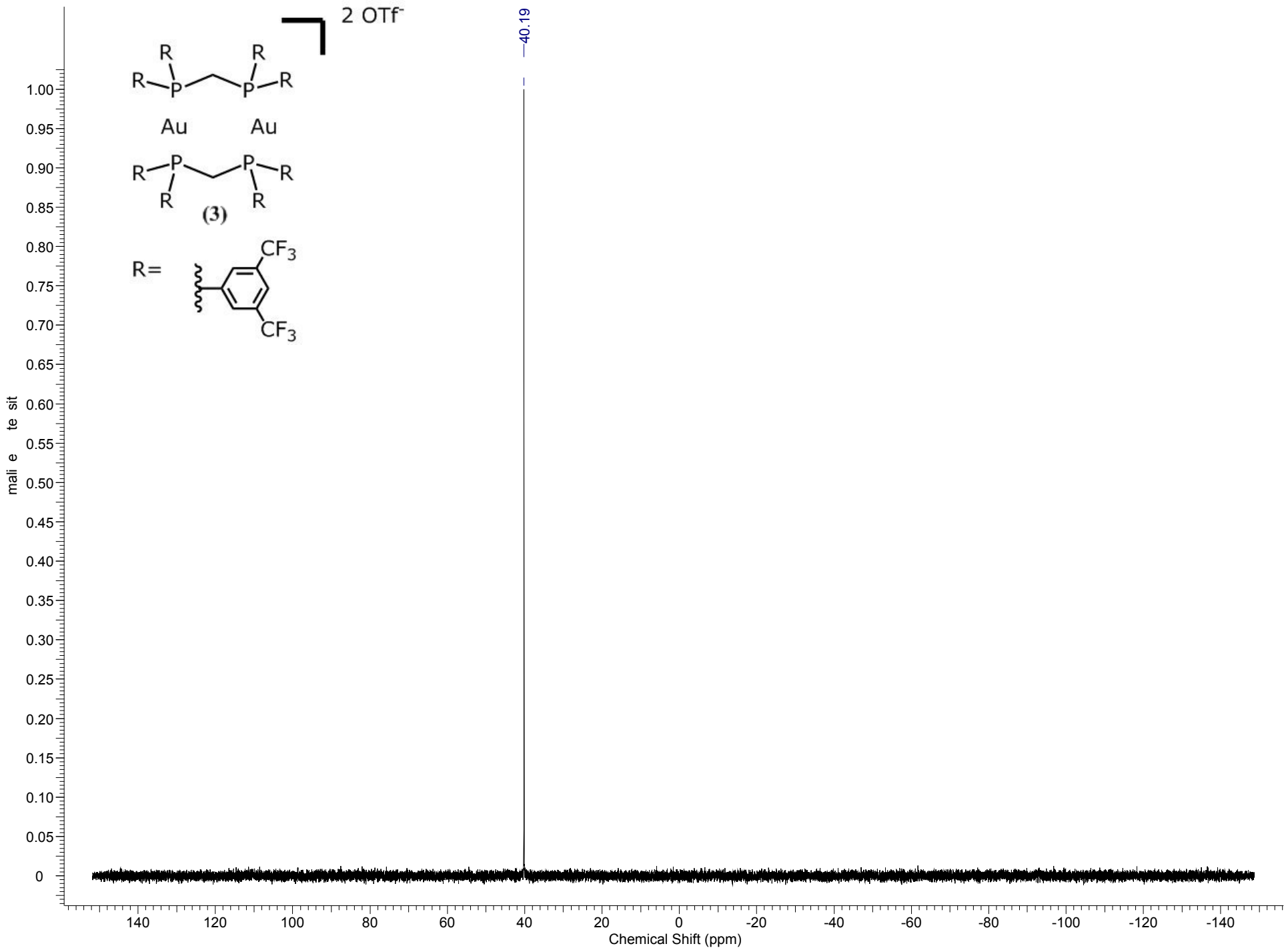
2 OTf-
40.19
Au
Au
(3)
R=
CF3
CF3
mali e te sit
1.00
0.95
0.90
0.85
0.80
0.75
0.70
0.65
0.60
0.55
0.50
0.45
0.40
0.35
0.30
0.25
0.20
0.15
0.10
0.05
0
140
120
100
80
60
40
20
0
-20
-40
-60
-80
-100
-120
-140
Chemical Shift (ppm)

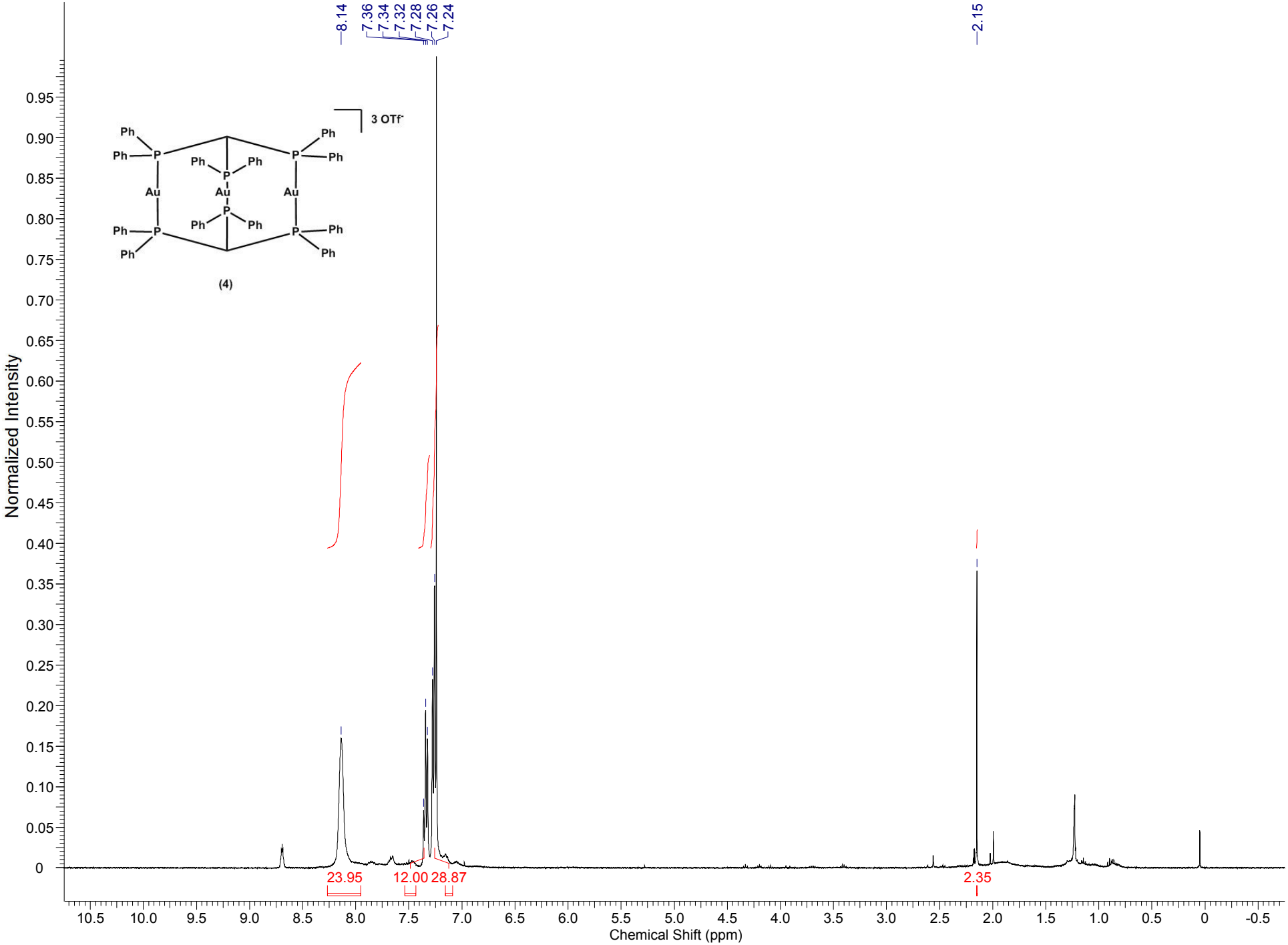
8.14
7.36
7.34
7.32
7.28
7.26
7.24
2.15
3 OTf⁻
Ph
P
Au
(4)
Normalized Intensity
Chemical Shift (ppm)
23.95
12.00
28.87
2.35

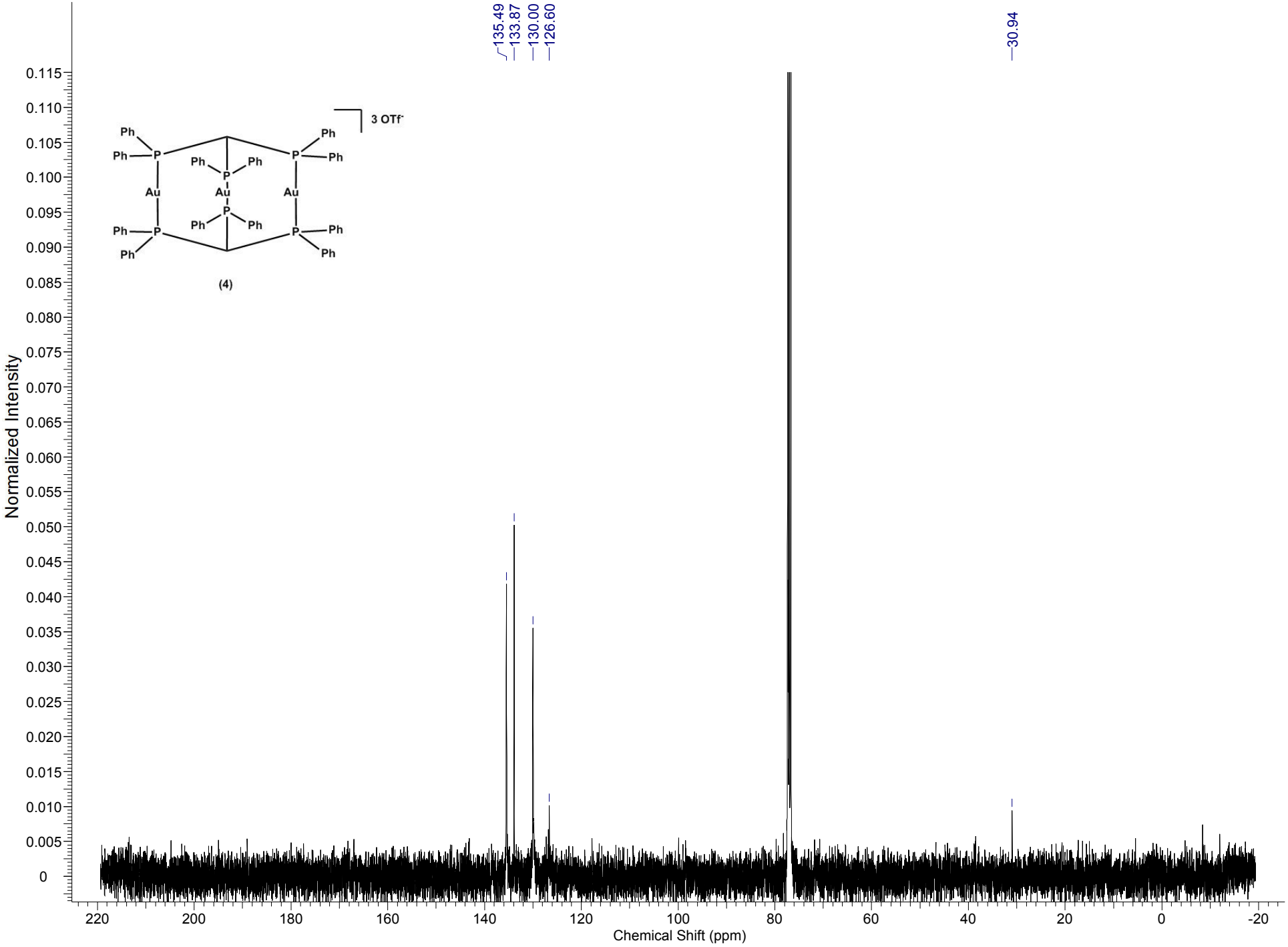
135.49
133.87
130.00
126.60
30.94
3 OTf-
(4)
Normalized Intensity
Chemical Shift (ppm)

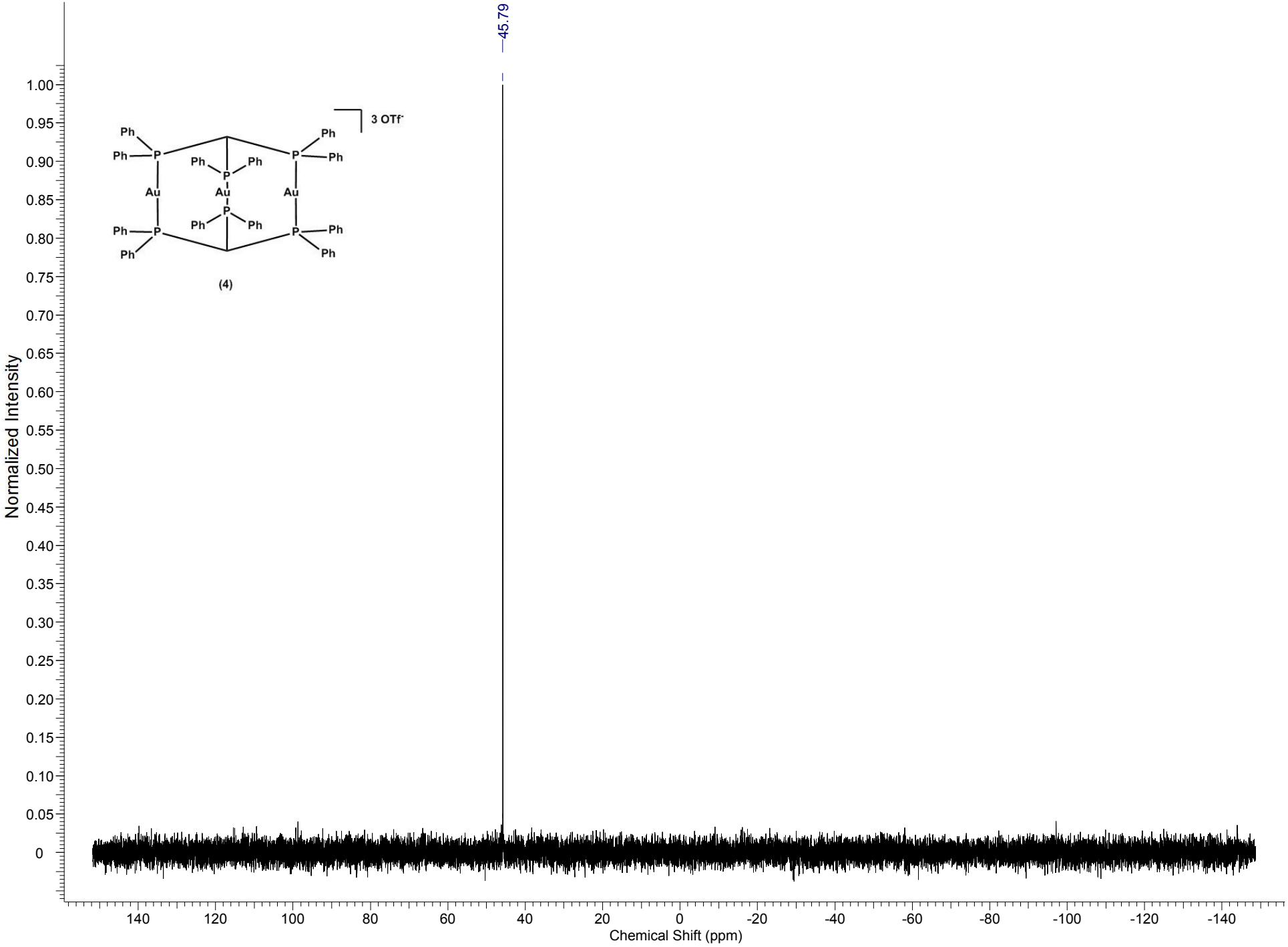
45.79
3 OTf-
Ph
P
Au
(4)
Normalized Intensity
1.00
0.95
0.90
0.85
0.80
0.75
0.70
0.65
0.60
0.55
0.50
0.45
0.40
0.35
0.30
0.25
0.20
0.15
0.10
0.05
0
140
120
100
80
60
40
20
0
-20
-40
-60
-80
-100
-120
-140
Chemical Shift (ppm)

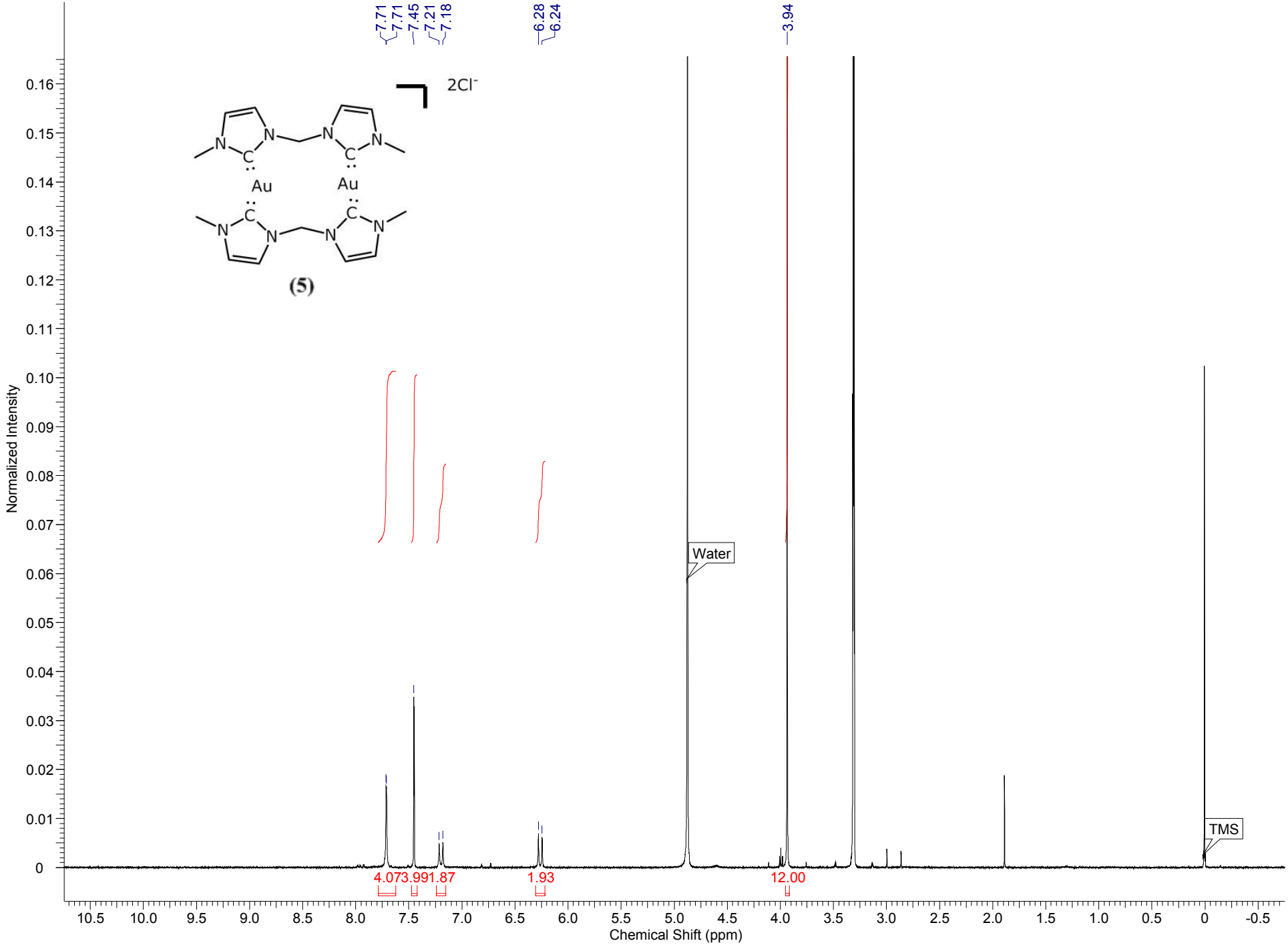
7.71
7.71
7.45
7.21
7.18
6.28
6.24
3.94
2Cl⁻
Au
Au
(5)
Water
TMS
4.07
3.99
1.87
1.93
12.00
Normalized Intensity
Chemical Shift (ppm)

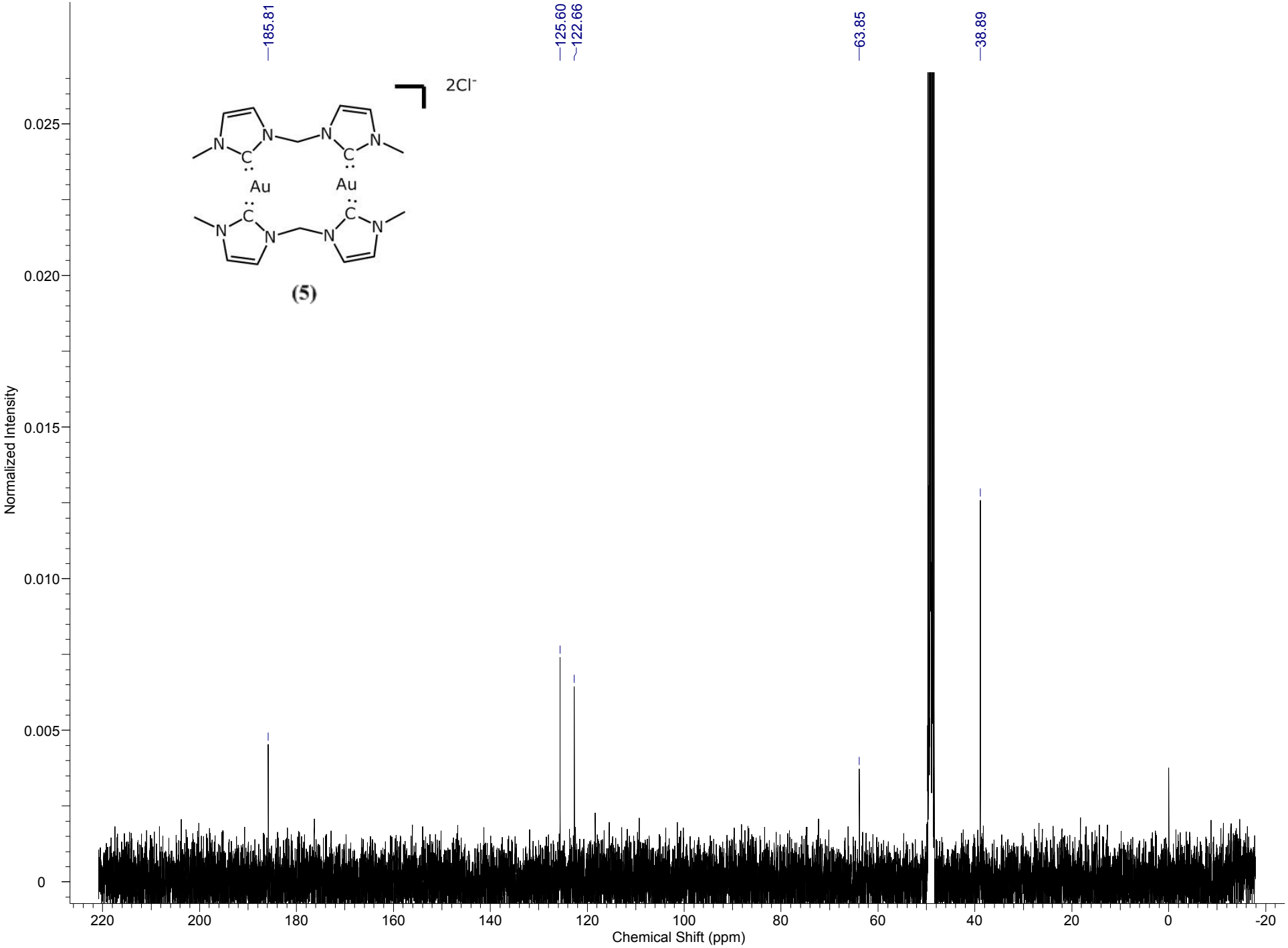
185.81
125.60
122.66
63.85
38.89
2Cl⁻
Au
Au
(5)
Normalized Intensity
0.025
0.020
0.015
0.010
0.005
0
220
200
180
160
140
120
100
80
60
40
20
0
-20
Chemical Shift (ppm)

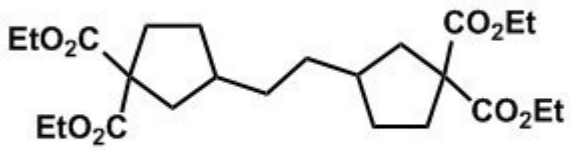

7b

4.18 4.17 4.16 4.15 4.13 2.42 2.41 2.39 2.27 2.12 2.12 1.87 1.86 1.85 1.66 1.65 1.33 1.32 1.32 1.24 1.23 1.21

8.00 1.97 2.06 2.08 3.96 1.98 3.99 14.07

mali e te it

Chemical Shift (ppm)

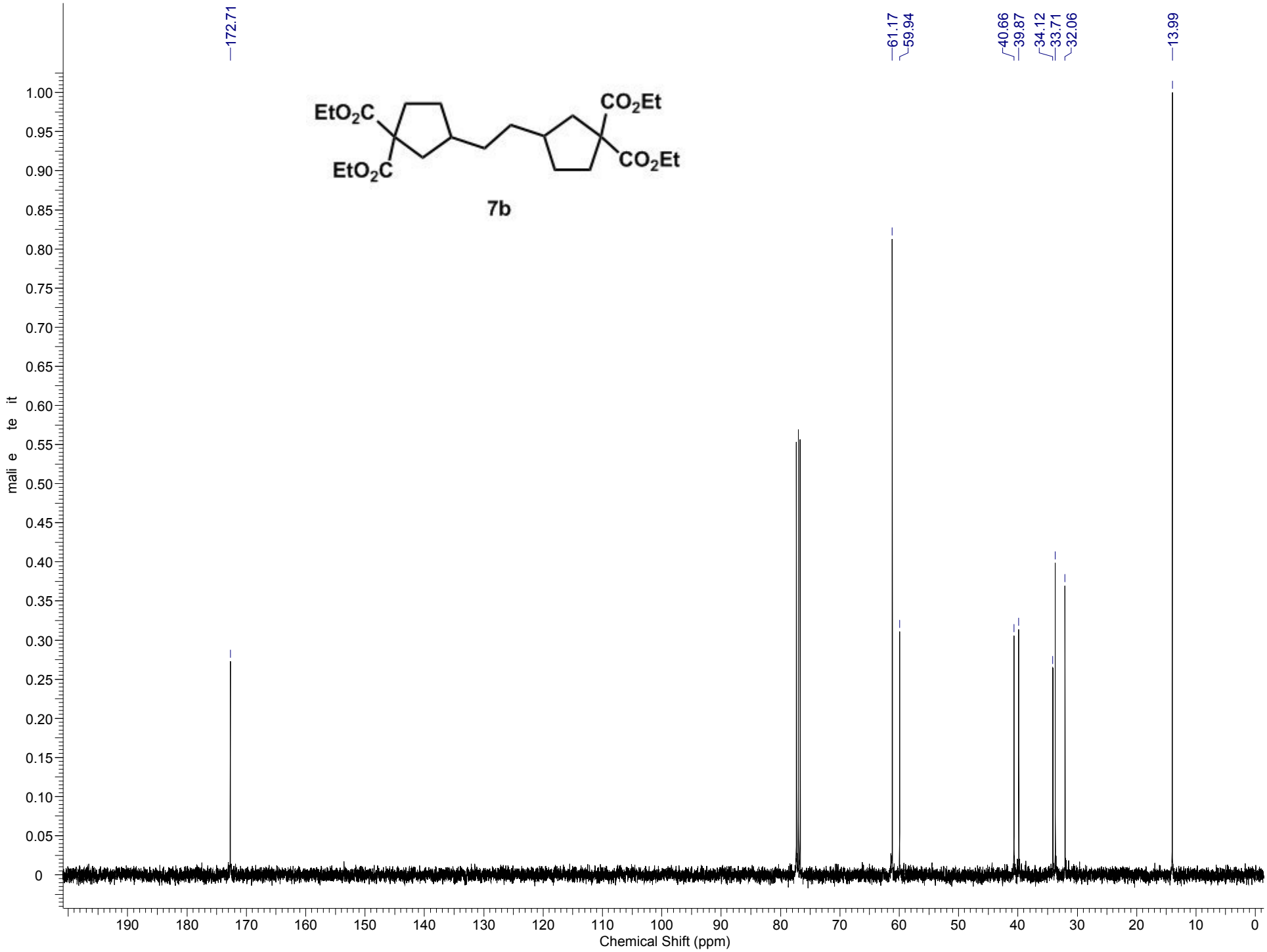
172.71
61.17
59.94
40.66
39.87
34.12
33.71
32.06
13.99
EtO2C
EtO2C
CO2Et
CO2Et
7b
mali e te it
Chemical Shift (ppm)

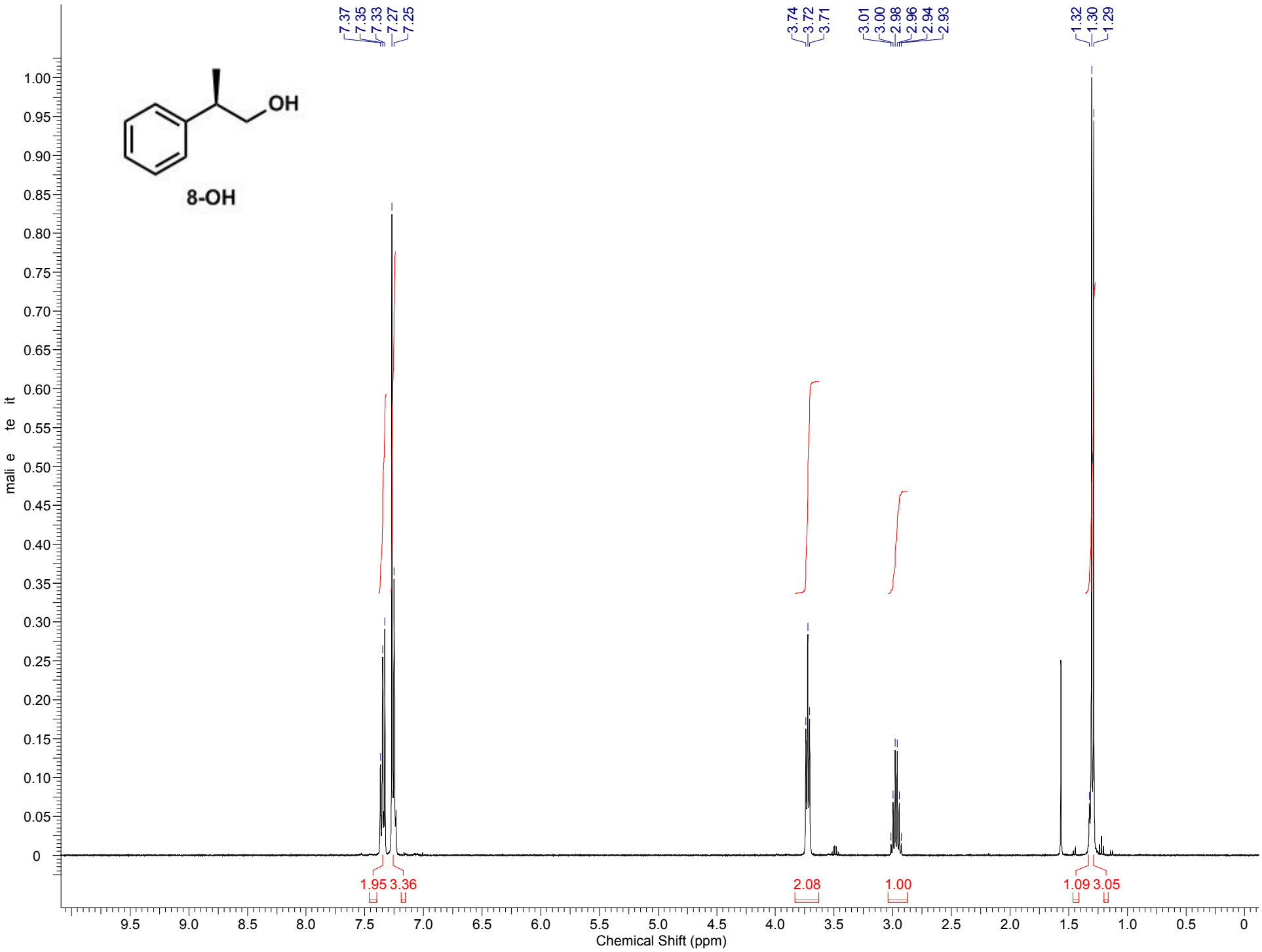
7.37
7.35
7.33
7.27
7.25
3.74
3.72
3.71
3.01
3.00
2.98
2.96
2.94
2.93
1.32
1.30
1.29
OH
8-OH
mali e te it
1.95
3.36
2.08
1.00
1.09
3.05
Chemical Shift (ppm)

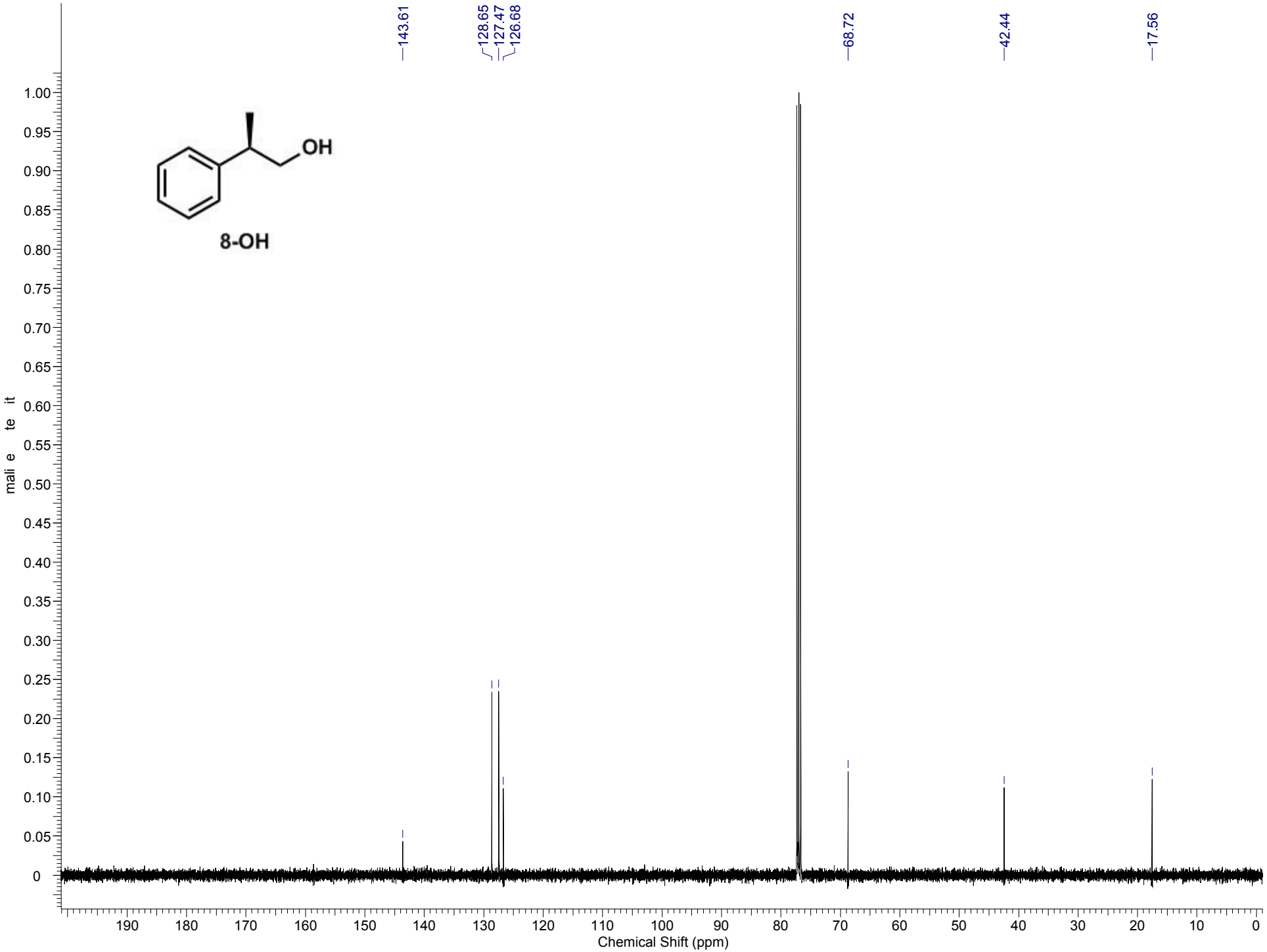
143.61
128.65
127.47
126.68
68.72
42.44
17.56
OH
8-OH
mali e te it
1.00
0.95
0.90
0.85
0.80
0.75
0.70
0.65
0.60
0.55
0.50
0.45
0.40
0.35
0.30
0.25
0.20
0.15
0.10
0.05
0
190
180
170
160
150
140
130
120
110
100
90
80
70
60
50
40
30
20
10
0
Chemical Shift (ppm)

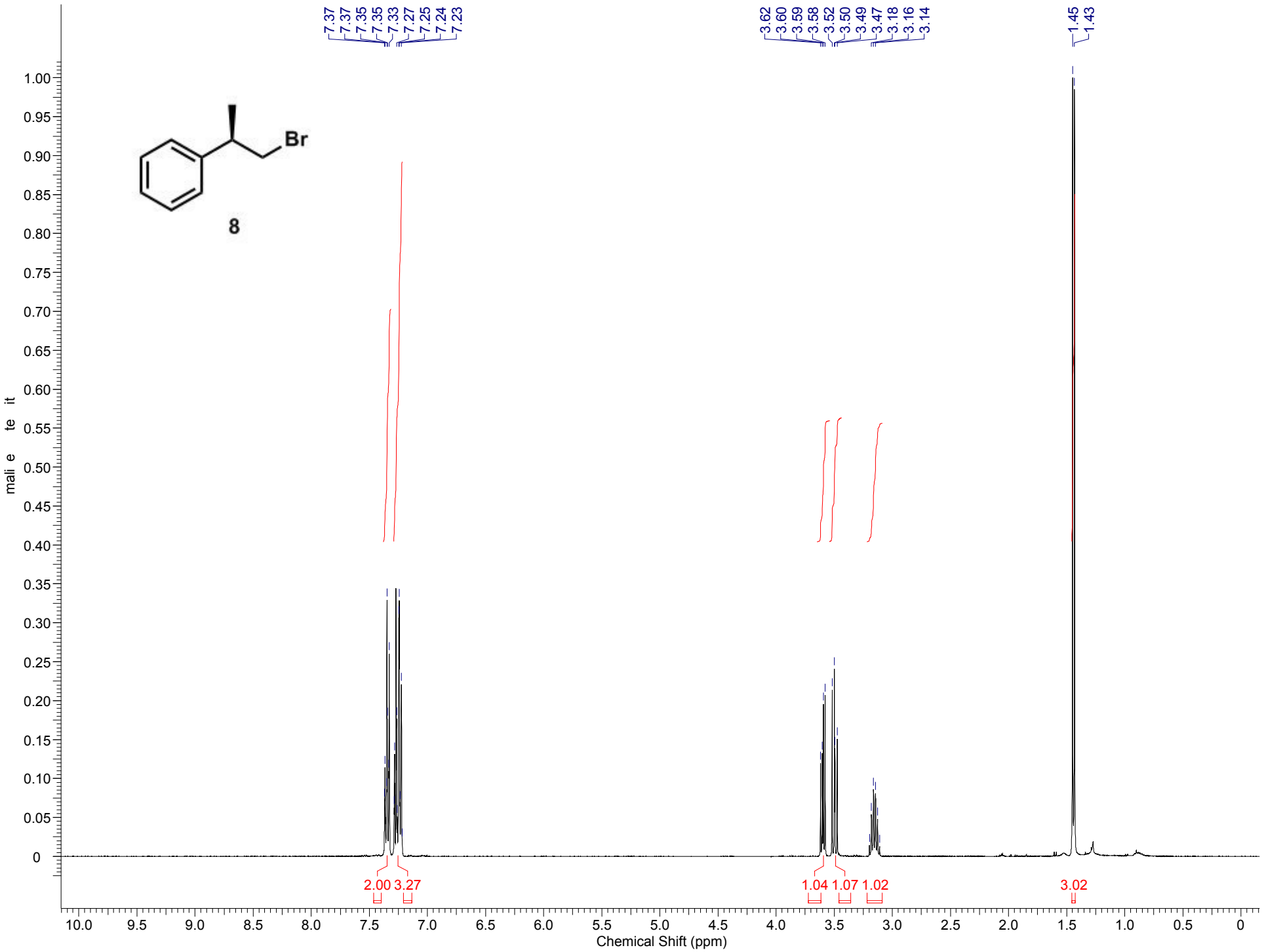
7.37
7.37
7.35
7.35
7.33
7.27
7.25
7.24
7.23
3.62
3.60
3.59
3.58
3.52
3.50
3.49
3.47
3.18
3.16
3.14
1.45
1.43
Br
8
mali e te it
2.00 3.27
1.04 1.07 1.02
3.02
Chemical Shift (ppm)

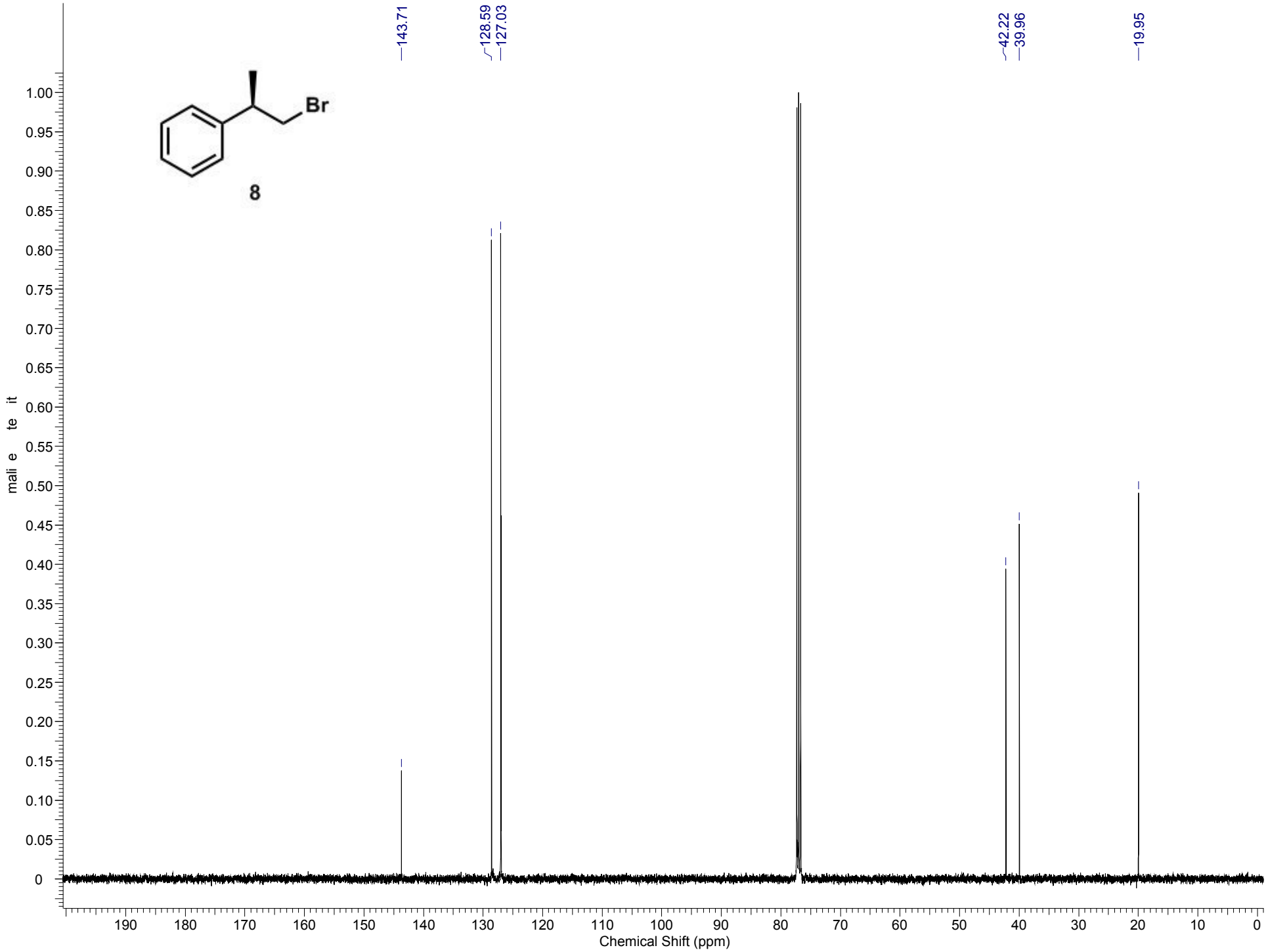
143.71
128.59
127.03
42.22
39.96
19.95
Br
8
mali e te it
Chemical Shift (ppm)